Research Article

Yongseok Jang and Simon Shaw*

A Priori Analysis of a Symmetric Interior Penalty Discontinuous Galerkin Finite Element Method for a Dynamic Linear Viscoelasticity Model

Abstract: The stress-strain constitutive law for viscoelastic materials such as soft tissues, metals at high temperature, and polymers, can be written as a Volterra integral equation of the second kind with a *fading memory* kernel. This integral relationship yields current stress for a given strain history and can be used in the momentum balance law to derive a mathematical model for the resulting deformation. We consider such a dynamic linear viscoelastic model problem resulting from using a *Dirichlet-Prony* series of decaying exponentials to provide the fading memory in the Volterra kernel. We introduce two types of *internal variable* to replace the Volterra integral with a system of auxiliary ordinary differential equations and then use a spatially discontinuous symmetric interior penalty Galerkin (SIPG) finite element method and — in time — a Crank-Nicolson method to formulate the fully discrete problems: one for each type of internal variable. We present *a priori* stability and error analyses without using Grönwall's inequality, and with the result that the constants in our estimates grow linearly with time rather than exponentially. In this sense the schemes are therefore suited to simulating long time viscoelastic response and this (to our knowledge) is the first time that such high quality estimates have been presented for SIPG finite element approximation of dynamic viscoelasticty problems. We also carry out a number of numerical experiments using the FEniCS environment (e.g. https://fenicsproject.org), describe a simulation using 'real' material data, and explain how the codes can be obtained and all of the results reproduced.

Keywords: Viscoelasticity, Generalised Maxwell Solid, Symmetric Interior Penalty, Discontinuous Galerkin Finite Element Method, *A priori* analysis, Internal variables

MSC 2010: 45D05, 65N12, 74D05, 74S05.

1 Introduction

The application of a *nonsymmetric interior penalty Discontinuous Galerkin* (NIPG) *Finite Element Method* (DGFEM) to a dynamic linear solid viscoelasticity problem with tensor-valued internal variable stress representation was presented by Rivière, Shaw and Whiteman in [22]. They gave an *a priori* energy error estimate by using the standard Grönwall inequality to deal with the time accumulation of error, and hence the constants in the stability and error bounds are too large to give confidence in the long time simulation

Yongseok Jang, ONERA Centre de Chatillon, 29 avenue de la Division Leclerc, 92322, Chatillon, France, Email: yongseok.jang@onera.fr

*Corresponding author: Simon Shaw, Department of Mathematics, Brunel University London, Kingston Lane, Uxbridge, UB8 3PH, UK, Email: simon.shaw@brunel.ac.uk

of viscoelastic response. In this paper, we use the symmetric interior penalty Galerkin (SIPG) method and prove stability bounds and *a priori* error estimates (not only in the energy norm but also in the spatial L_2 norm) without the use of Grönwall's inequality. We therefore obtain non-exponentially increasing bounds for temporal L_∞-type norms. Furthermore, we introduce vector-valued internal variables in *displacement form* and *velocity form* (to be defined below). This has the advantage of reducing computer memory requirements in that we need only store vectors of dimension d, instead of symmetric second order tensors of dimension $d(d+1)/2$, as in [22]. This can be significant for high fidelity 3D simulations.

We consider a linear homogeneous and isotropic viscoelastic solid material, e.g. [12], occupying a bounded polytopic domain, the interior of which is denoted by $\Omega \subset \mathbb{R}^d$, and consider the deformation and stress-strain state of this material over times $t \in [0, T]$, where $T > 0$. The deformation, $\boldsymbol{u}$, and stress, $\underline{\boldsymbol{\sigma}}$, follow the momentum equation,

$$\rho \ddot{\boldsymbol{u}} - \nabla \cdot \underline{\boldsymbol{\sigma}} = \boldsymbol{f} \qquad \text{on } \Omega \times (0, T], \tag{1.1}$$

where overdots denote time differentiation so that $\ddot{\boldsymbol{u}}$ is acceleration, ρ is the mass density of the material (assumed constant), $\nabla \cdot \underline{\boldsymbol{\sigma}}$ is the divergence of stress and $\boldsymbol{f}$ is an external body force (e.g. see [22, 23]). Similarly, $\dot{\boldsymbol{u}}$ denotes velocity. In addition to this vector-valued governing equation, we assume a mix of essential and natural boundary conditions so that

$$\boldsymbol{u}(t) = 0 \qquad \text{on } \Gamma_D \times [0, T], \tag{1.2}$$

$$\underline{\boldsymbol{\sigma}}(t) \cdot \boldsymbol{n} = \boldsymbol{g}_N(t) \qquad \text{on } \Gamma_N \times [0, T], \tag{1.3}$$

where Γ_D is the *Dirichlet* boundary (assumed to have positive surface measure), Γ_N is the *Neumann* boundary given by $\Gamma_N = \partial\Omega \backslash \Gamma_D$, $\boldsymbol{n}$ is an outward unit normal vector defined a.e. on Γ_N, and $\boldsymbol{g}_N$ prescribes a surface traction on Γ_N. Furthermore, for initial conditions on the displacement and the velocity we take,

$$\boldsymbol{u}(0) = \boldsymbol{u}_0 \qquad \text{and} \qquad \dot{\boldsymbol{u}}(0) = \boldsymbol{w}_0 \tag{1.4}$$

for given functions $\boldsymbol{u}_0$ and $\boldsymbol{w}_0$.

To close the problem, and solve for displacement, we need a constitutive equation expressing stress in terms of displacement. In the linear viscoelasticity model considered here this involves a Volterra (or 'fading memory') integral with the specific material characterised by stiffness, $\underline{\boldsymbol{D}}$, and a stress relaxation function, φ, see e.g. [8, 10, 15, 23, 12]. The stress is then given by

$$\underline{\boldsymbol{\sigma}}(t) = \underline{\boldsymbol{D}}\varphi(t)\underline{\boldsymbol{\varepsilon}}(0) + \int_0^t \underline{\boldsymbol{D}}\varphi(t-s)\dot{\underline{\boldsymbol{\varepsilon}}}(s)ds, \tag{1.5}$$

where $\underline{\boldsymbol{D}}$ is a fourth order positive definite tensor satisfying the symmeteries $D_{ijkl} = D_{jikl} = D_{ijlk} = D_{klij}$, and $\underline{\boldsymbol{\varepsilon}}$ is the strain defined by

$$\varepsilon_{ij}(\boldsymbol{v}) = \frac{1}{2}\left(\frac{\partial v_i}{\partial x_j} + \frac{\partial v_j}{\partial x_i}\right), \qquad \text{for } i, j = 1, \ldots, d.$$

Note that in (1.5) we use the shorthand $\underline{\boldsymbol{\varepsilon}}(t) = \underline{\boldsymbol{\varepsilon}}(\boldsymbol{u}(t))$. The form of φ depends on which viscoelastic model is invoked. There are several (see e.g. [8, 10, 12] and the references therein) but here we focus on the *Generalised Maxwell solid* where

$$\varphi(t) = \varphi_0 + \sum_{q=1}^{N_\varphi} \varphi_q e^{-t/\tau_q} \tag{1.6}$$

with $N_\varphi \in \mathbb{N}$, strictly positive delay times $\{\tau_q\}_{q=1}^{N_\varphi}$, and coefficients $\{\varphi_q\}_{q=0}^{N_\varphi}$ the latter of which are normalised so that $\varphi(0) = 1$. The positivity requirement excludes the case $\varphi_0 = 0$ (a fluid in the sense used

by Golden and Graham in [12]): this is an important assumption in the arguments developed below. In particular, in moving from (4.4) to (4.5) we will use the fact that

$$1 - \sum_{q=1}^{N_\varphi} \varphi_q = \varphi(0) - \sum_{q=1}^{N_\varphi} \varphi_q = \varphi_0 > 0. \tag{1.7}$$

This paper is arranged as follows. In Section 2 we give our notations and the preliminary background for DGFEM. In Section 3 we introduce two forms of internal variables, each of which are used to represent the Volterra (or 'history') integral, and formulate a variational problem for each form. We then state and prove (without using Grönwall's inequality) stability bounds in Section 4 and error bounds in Section 5, carry out some illustrative numerical experiments in Section 6, using FEniCS, see [1] and https://fenicsproject.org, and then end with some concluding remarks in Section 7.

2 Preliminary

We use standard notation so that $L_p(\Omega)$, $H^s(\Omega)$ and $W_p^s(\Omega)$ (with s and p non-negative) denote the usual Lebesgue, Hilbert and Sobolev spaces. For any normed space X, $\|\cdot\|_X$ is the X norm which, for inner product spaces, is always the norm induced by the inner product. For example, $\|\cdot\|_{L_2(\Omega)}$ is the $L_2(\Omega)$ norm, as induced by the $L_2(\Omega)$ inner product denoted—for brevity—by $(\cdot, \cdot)$, but for $S \subset \bar{\Omega}$, we use $(\cdot, \cdot)_{L_2(S)}$ for the $L_2(S)$ inner product. For time dependent functions we expand this notation so that for X a normed target space, $f \in L_p(0, T; X)$ denotes the space of $L_p(0, T) \to X$ functions with norm

$$\|f\|_{L_p(0,T;X)} = \left(\int_0^T \|f(t)\|_X^p \, dt \right)^{1/p},$$

for $1 \leqslant p < \infty$. When $p = \infty$ this becomes the *essential supremum* norm:

$$\|f\|_{L_\infty(0,T;X)} = \operatorname*{ess\,sup}_{0 \leqslant t \leqslant T} \|f(t)\|_X.$$

When convenient, we shall often replace the upper limit T in these expressions by some other value $t \in [0, T]$.

For inner products of vector-valued and tensor-valued functions we use the same notation as for the scalar cases. For instance, we have

$$(\boldsymbol{v}, \boldsymbol{w}) = \int_\Omega \boldsymbol{v} \cdot \boldsymbol{w} \, d\Omega, \qquad (\underline{\boldsymbol{v}}, \underline{\boldsymbol{w}}) = \int_\Omega \underline{\boldsymbol{v}} : \underline{\boldsymbol{w}} \, d\Omega = \sum_{i,j=1}^d \int_\Omega v_{ij} w_{ij} \, d\Omega,$$

for vector-valued functions $\boldsymbol{v}$ and $\boldsymbol{w}$, and second order tensors $\underline{\boldsymbol{v}}$ and $\underline{\boldsymbol{w}}$.

Meshes

We refer to [20] for a detailed explanation of the framework of the DGFEM and here just summarise the main points. Assume that the closure of Ω is subdivided into closed elements E, where E is a triangle in 2D or a tetrahedron in 3D, and the intersection of any pair of elements is either a vertex, an edge, a face, or empty. The diameter of E is defined by $h_E := \sup_{x,y \in E} \|x - y\|$, where $\|\cdot\|$ is the Euclidean norm, and $|E|$ denotes the measure (area/volume) of E. In a similar way, let e be an edge of E and use $|e|$ to denote its measure (length/area). Let h be the maximum of the diameters h_E over all the elements E, and define the set $\mathcal{E}_h$ of all of those elements. Then $|e| \leqslant h_E^{d-1} \leqslant h^{d-1}$ for all $e \subset \partial E$ for each $E \in \mathcal{E}_h$. We further suppose that the subdivision is quasi-uniform, which means that there exists a positive constant C such that $h \leqslant C h_E$ for all $E \in \mathcal{E}_h$.

Next, let Γ_h be the set of interior edges (in 2D) or faces (in 3D) contained in the subdivision $\mathcal{E}_h$. Then for each edge or face element e, we can define a unit normal vector, $\boldsymbol{n}_e$. If $e \subset \partial\Omega$, $\boldsymbol{n}_e$ is the outward unit normal vector. For an interior edge e such that $e \subset E_i \cap E_j$ with $i < j$, the normal vector $\boldsymbol{n}_e$ is oriented from E_i to E_j.

Test spaces

We introduce the broken Sobolev space $H^s(\mathcal{E}_h) = \{v \in L_2(\Omega) \mid \forall E \in \mathcal{E}_h, \ v|_E \in H^s(E)\}$ and endow it with the broken Sobolev norm, $\|\|\cdot\|\|_{H^s(\mathcal{E}_h)}$, defined by

$$\|\|v\|\|_{H^s(\mathcal{E}_h)} = \left(\sum_{E \in \mathcal{E}_h} \|v\|^2_{H^s(E)} \right)^{1/2}.$$

We note the following facts $H^s(\Omega) \subset H^s(\mathcal{E}_h)$ and $H^{s+1}(\mathcal{E}_h) \subset H^s(\mathcal{E}_h)$. These definitions and notations are extended in an obvious way to the the vector field analogue $\boldsymbol{H}^s(\mathcal{E}_h)$.

We define the space of polynomials of degree less than or equal to k on E, for $E \subset \mathbb{R}^d$, by

$$\mathcal{P}_k(E) = \text{span}\left\{ x_1^{i_1} \cdots x_d^{i_d} \mid \sum_{m=1}^{d} i_m \leqslant k, \ \boldsymbol{x} \in E, i_m \in \mathbb{N} \cup \{0\} \text{ for each } m \right\},$$

and then define our DG finite element space as

$$\mathcal{D}_k(\mathcal{E}_h) = \{v \in H^1(\mathcal{E}_h) \mid v|_E \in \mathcal{P}_k(E) \text{ for each } E \in \mathcal{E}_h\}.$$

The analogous vector field is given by $\boldsymbol{\mathcal{D}}_k(\mathcal{E}_h) := [\mathcal{D}_k(\mathcal{E}_h)]^d$.

Average and Jump

Suppose two elements E_i^e and E_j^e share the common edge e with $i < j$ and that there is a vector valued function $\boldsymbol{v}$ and a second order tensor $\underline{\boldsymbol{v}}$ on E_i^e and E_j^e. Then we define an average and a jump for $\boldsymbol{v}$ and $\underline{\boldsymbol{v}}$ by

$$\{\boldsymbol{v}\} = \frac{(\boldsymbol{v}|_{E_i^e})|_e + (\boldsymbol{v}|_{E_j^e})|_e}{2}, \qquad \{\underline{\boldsymbol{v}}\} = \frac{(\underline{\boldsymbol{v}}|_{E_i^e})|_e + (\underline{\boldsymbol{v}}|_{E_j^e})|_e}{2},$$

$$[\boldsymbol{v}] = (\boldsymbol{v}|_{E_i^e})|_e - (\boldsymbol{v}|_{E_j^e})|_e, \qquad [\boldsymbol{v} \otimes \boldsymbol{n}_e] = (\boldsymbol{v}|_{E_i^e})|_e \otimes \boldsymbol{n}_e - (\boldsymbol{v}|_{E_j^e})|_e \otimes \boldsymbol{n}_e,$$

where the normal vector $\boldsymbol{n}_e$ is oriented from E_i^e to E_j^e and $\otimes$ is the outer product defined, for vectors $\boldsymbol{a}$ and $\boldsymbol{b}$, by $(\boldsymbol{a} \otimes \boldsymbol{b})_{mn} = a_m b_n$ for $m, n = 1, \ldots, d$. On the other hand, if $e \subset \partial\Omega$ and $e \subset \partial E$

$$\{\boldsymbol{v}\} = \boldsymbol{v}|_e, \qquad \{\underline{\boldsymbol{v}}\} = \underline{\boldsymbol{v}}|_e, \qquad [\boldsymbol{v}] = \boldsymbol{v}|_e \cdot \boldsymbol{n}_e, \qquad \text{and} \qquad [\boldsymbol{v} \otimes \boldsymbol{n}_e] = \boldsymbol{v}|_e \otimes \boldsymbol{n}_e.$$

We can now introduce the jump penalty operator,

$$J_0^{\alpha_0, \beta_0}(\boldsymbol{v}, \boldsymbol{w}) = \sum_{e \subset \Gamma_h \cup \Gamma_D} \frac{\alpha_0}{|e|^{\beta_0}} \int_e [\boldsymbol{v}] \cdot [\boldsymbol{w}] \, de,$$

where α_0 and β_0 are positive constants.

Useful inequalities

We now recall the following inequalities for use later in the *a priori* analysis.

– Inverse polynomial trace inequalities [24]: For any $v \in \mathcal{P}_k(E)$, $\forall e \subset \partial E$,

$$\begin{cases} \|v\|_{L_2(e)} & \leqslant C|e|^{1/2}|E|^{-1/2}\|v\|_{L_2(E)}, \\ \|v\|_{L_2(e)} & \leqslant C h_E^{-1/2}\|v\|_{L_2(E)}, \\ \|\nabla v \cdot \boldsymbol{n}_e\|_{L_2(e)} & \leqslant C|e|^{1/2}|E|^{-1/2}\|\nabla v\|_{L_2(E)}, \\ \|\nabla v \cdot \boldsymbol{n}_e\|_{L_2(e)} & \leqslant C h_E^{-1/2}\|\nabla v\|_{L_2(E)}, \end{cases} \qquad (2.1)$$

where C is a positive constant and is independent of h_E but depends on the polynomial degree k.

– Poincaré's Inequality [3, 20]: If $\beta_0(d-1) \geqslant 1$ and $|e| \leqslant 1$ for every $e \subset \Gamma_h \cup \Gamma_D$, then,

$$\left\| v \right\|_{L_2(\Omega)} \leqslant C \left(\left\| \nabla v \right\|^2_{H^0(\mathcal{E}_h)} + \sum_{e \subset \Gamma_h \cup \Gamma_D} \frac{1}{|e|^{\beta_0}} \left\| [v] \right\|^2_{L_2(e)} \right)^{1/2}, \tag{2.2}$$

for any $v \in H^1(\mathcal{E}_h)$.

– Inverse Inequality (or Markov Inequality) [18, 20]: For any $E \in \mathcal{E}_h$, there is a positive constant C such that

$$\forall v \in \mathcal{P}_k(E), \ \left\| \nabla^j v \right\|_{L_2(E)} \leqslant C h_E^{-j} \left\| v \right\|_{L_2(E)}, \ \forall j \in \{0, 1, \ldots, k\}, \tag{2.3}$$

where

$$\nabla^j v = \begin{cases} \nabla \cdot \nabla^{j-1} v & \text{for even } j, \\ \nabla(\nabla^{j-1} v) & \text{for odd } j, \end{cases} \quad \text{and} \quad \nabla^0 v = v.$$

Note that these three inequalities can also be applied in the obvious way to vector-valued functions.

DG bilinear form

We define a DG bilinear form $a : \boldsymbol{H}^s(\mathcal{E}_h) \times \boldsymbol{H}^s(\mathcal{E}_h) \mapsto \mathbb{R}$ for $s > 3/2$ by

$$a(\boldsymbol{v}, \boldsymbol{w}) = \sum_{E \in \mathcal{E}_h} \int_E \underline{\boldsymbol{D}} \underline{\boldsymbol{\varepsilon}}(\boldsymbol{v}) : \underline{\boldsymbol{\varepsilon}}(\boldsymbol{w}) \, dE - \sum_{e \subset \Gamma_h \cup \Gamma_D} \int_e \{\underline{\boldsymbol{D}} \underline{\boldsymbol{\varepsilon}}(\boldsymbol{v})\} : [\boldsymbol{w} \otimes \boldsymbol{n}_e] \, de$$
$$- \sum_{e \subset \Gamma_h \cup \Gamma_D} \int_e \{\underline{\boldsymbol{D}} \underline{\boldsymbol{\varepsilon}}(\boldsymbol{w})\} : [\boldsymbol{v} \otimes \boldsymbol{n}_e] \, de + J_0^{\alpha_0, \beta_0}(\boldsymbol{v}, \boldsymbol{w}), \tag{2.4}$$

for any $\boldsymbol{v}, \boldsymbol{w} \in \boldsymbol{H}^s(\mathcal{E}_h)$. We also define our DG energy norm by

$$\left\| \boldsymbol{v} \right\|_V = \left(\sum_{E \in \mathcal{E}_h} \int_E \underline{\boldsymbol{D}} \underline{\boldsymbol{\varepsilon}}(\boldsymbol{v}) : \underline{\boldsymbol{\varepsilon}}(\boldsymbol{v}) \, dE + J_0^{\alpha_0, \beta_0}(\boldsymbol{v}, \boldsymbol{v}) \right)^{1/2}, \quad \text{for } \boldsymbol{v} \in \boldsymbol{H}^s(\mathcal{E}_h). \tag{2.5}$$

Comparing these we can observe that

$$a(\boldsymbol{v}, \boldsymbol{v}) = \left\| \boldsymbol{v} \right\|_V^2 - 2 \sum_{e \subset \Gamma_h \cup \Gamma_D} \int_e \{\underline{\boldsymbol{D}} \underline{\boldsymbol{\varepsilon}}(\boldsymbol{v})\} : [\boldsymbol{v} \otimes \boldsymbol{n}_e] \, de. \tag{2.6}$$

Remark 2.1. *In the DG bilinear form, the third term is called the "interior penalty" term and the last one is called the "jump penalty". Depending on the sign of the interior penalty, the bilinear form is either symmetric or nonsymmetric. In this article, we consider only the symmetric DG method and refer to [16, 22] for an application of the nonsymmetric method for viscoelasticity. The reason why we employ SIPG is that it requires only the standard penalisation, $\beta_0(d-1) \geqslant 1$, for optimal spatial error estimates, while NIPG needs the super penalisation $\beta_0(d-1) \geqslant 3$. Since the use of the super penalisation enforces the linear system to be more ill-conditioned, we may encounter some difficulty in solving the system with iterative solvers. For more details, we refer to [16].*

Remark 2.2 (Korn's inequality for piecewise H^1 vector fields [4, 20])**.** *If we have $\beta_0(d-1) \geqslant 1$, then since $\underline{\boldsymbol{D}}$ is symmetric positive definite and the jump penalty is defined not only on the interior edges but also on the positive measured Dirichlet boundary, Korn's inequality yields, for any $\boldsymbol{v} \in \boldsymbol{H}^1(\mathcal{E}_h)$,*

$$\sum_{E \in \mathcal{E}_h} \left\| \nabla \boldsymbol{v} \right\|^2_{L_2(E)} \leqslant C \left\| \boldsymbol{v} \right\|_V^2, \tag{2.7}$$

for some positive C independent of $\boldsymbol{v}$.

In CGFEM the squared energy norm, $\|\boldsymbol{v}\|_V^2$, is usually given by the energy inner product, $a(\boldsymbol{v}, \boldsymbol{v})$. Here, in DGFEM, we see from (2.6) that this is nearly true but there is an extra term. The following lemma allows us to deal with that term.

Lemma 2.1. *Suppose $\alpha_0 > 0$ and $\beta_0(d-1) \geqslant 1$. For any $\boldsymbol{v}, \boldsymbol{w} \in \boldsymbol{\mathcal{D}}_k(\mathcal{E}_h)$, and for any pair $E_1, E_2 \in \mathcal{E}_h$, we have*

$$\left| \int_e \{\underline{\boldsymbol{D}}\underline{\varepsilon}(\boldsymbol{v})\} : [\boldsymbol{w} \otimes \boldsymbol{n}_e] \, de \right| \leqslant \frac{C}{\sqrt{\alpha_0}} \left(\|\underline{\boldsymbol{D}}\underline{\varepsilon}(\boldsymbol{v})\|_{L_2(E_1)}^2 + \|\underline{\boldsymbol{D}}\underline{\varepsilon}(\boldsymbol{v})\|_{L_2(E_2)}^2 + \frac{\alpha_0}{|e|^{\beta_0}} \|[\boldsymbol{w}]\|_{L_2(e)}^2 \right), \qquad (2.8)$$

where e is the shared edge of elements E_1 and E_2, and C is a positive constant independent of $\boldsymbol{v}$ and $\boldsymbol{w}$ but dependent on the inverse polynomial trace inequality's constants and the domain. When $e \subset \partial\Omega$, (2.8) holds with $E_1 = E_2$.

Proof. Let $e \subset \Gamma_h$ and $e \subset E_1 \cap E_2$ where $E_1, E_2 \in \mathcal{E}_h$. Recalling the definitions of the average and jump, and using the Cauchy-Schwarz inequality, we have

$$\left| \int_e \{\underline{\boldsymbol{D}}\underline{\varepsilon}(\boldsymbol{v})\} : [\boldsymbol{w} \otimes \boldsymbol{n}_e] \, de \right| \leqslant \frac{1}{2} \left(\left\|\underline{\boldsymbol{D}}\underline{\varepsilon}(\boldsymbol{v}|_{E_1})\right\|_{L_2(e)} + \left\|\underline{\boldsymbol{D}}\underline{\varepsilon}(\boldsymbol{v}|_{E_2})\right\|_{L_2(e)} \right) \frac{|e|^{\beta_0/2}}{|e|^{\beta_0/2}} \|[\boldsymbol{w}]\|_{L_2(e)},$$

after noting that $[\boldsymbol{w} \otimes \boldsymbol{n}_e] = [\boldsymbol{w}] \otimes \boldsymbol{n}_e$, since $\boldsymbol{n}_e|_{E_1} = -\boldsymbol{n}_e|_{E_2}$. The inverse polynomial trace inequality (2.1) implies that

$$\left| \int_e \{\underline{\boldsymbol{D}}\underline{\varepsilon}(\boldsymbol{v})\} : [\boldsymbol{w} \otimes \boldsymbol{n}_e] \, de \right| \leqslant C \left(|e|^{\beta_0/2} h_{E_1}^{-1/2} \|\underline{\boldsymbol{D}}\underline{\varepsilon}(\boldsymbol{v})\|_{L_2(E_1)} + |e|^{\beta_0/2} h_{E_2}^{-1/2} \|\underline{\boldsymbol{D}}\underline{\varepsilon}(\boldsymbol{v})\|_{L_2(E_2)} \right) \frac{\left\|[\boldsymbol{w}]\right\|_{L_2(e)}}{|e|^{\beta_0/2}},$$

for a positive constant C. Since $|e| \leqslant h^{d-1}$, the discrete Cauchy-Schwarz inequality yields

$$\left| \int_e \{\underline{\boldsymbol{D}}\underline{\varepsilon}(\boldsymbol{v})\} : [\boldsymbol{w} \otimes \boldsymbol{n}_e] de \right|$$

$$\leqslant C \left(h_{E_1}^{\beta_0(d-1)-1} + h_{E_2}^{\beta_0(d-1)-1} \right)^{1/2} \left(\|\underline{\boldsymbol{D}}\underline{\varepsilon}(\boldsymbol{v})\|_{L_2(E_1)}^2 + \|\underline{\boldsymbol{D}}\underline{\varepsilon}(\boldsymbol{v})\|_{L_2(E_2)}^2 \right)^{1/2} \frac{\left\|[\boldsymbol{w}]\right\|_{L_2(e)}}{|e|^{\beta_0/2}},$$

$$\leqslant C \left(\|\underline{\boldsymbol{D}}\underline{\varepsilon}(\boldsymbol{v})\|_{L_2(E_1)}^2 + \|\underline{\boldsymbol{D}}\underline{\varepsilon}(\boldsymbol{v})\|_{L_2(E_2)}^2 \right)^{1/2} \frac{\left\|[\boldsymbol{w}]\right\|_{L_2(e)}}{|e|^{\beta_0/2}},$$

because $h_{E_1} \leqslant \operatorname{diam}(\Omega)$, $h_{E_2} \leqslant \operatorname{diam}(\Omega)$ and $\beta_0(d-1) \geqslant 1$. Using Young's inequality we then obtain

$$\left| \int_e \{\underline{\boldsymbol{D}}\underline{\varepsilon}(\boldsymbol{v})\} : [\boldsymbol{w} \otimes \boldsymbol{n}_e] de \right| \leqslant C \left(\frac{\epsilon}{2} \left(\|\underline{\boldsymbol{D}}\underline{\varepsilon}(\boldsymbol{v})\|_{L_2(E_1)}^2 + \|\underline{\boldsymbol{D}}\underline{\varepsilon}(\boldsymbol{v})\|_{L_2(E_2)}^2 \right) + \frac{1}{2\epsilon} \frac{\left\|[\boldsymbol{w}]\right\|_{L_2(e)}^2}{|e|^{\beta_0}} \right),$$

for any positive ϵ. Taking $\epsilon = 1/\sqrt{\alpha_0}$ then completes the proof. $\qquad \square$

Corollary 2.1. *By (2.8), we can also derive*

$$\sum_{e \subset \Gamma_h \cup \Gamma_D} \int_e \left| \{\underline{\boldsymbol{D}}\underline{\varepsilon}(\boldsymbol{v})\} : [\boldsymbol{w} \otimes \boldsymbol{n}_e] de \right| \leqslant \frac{C}{\sqrt{\alpha_0}} \left(\|\boldsymbol{v}\|_V^2 + J_0^{\alpha_0, \beta_0}(\boldsymbol{w}, \boldsymbol{w}) \right), \qquad (2.9)$$

where C is a positive constant independent of $\boldsymbol{v}, \boldsymbol{w} \in \boldsymbol{\mathcal{D}}_k(\mathcal{E}_h)$ but dependent on the inverse polynomial trace inequality's constant in (2.1).

Theorem 2.1 (Coercivity and continuity)**.** *Suppose $\alpha_0 > 0$ is sufficiently large and $\beta_0(d-1) \geqslant 1$. Then there exist positive constants κ and K such that*

$$\kappa \|\boldsymbol{v}\|_V^2 \leqslant a(\boldsymbol{v}, \boldsymbol{v}), \qquad |a(\boldsymbol{v}, \boldsymbol{w})| \leqslant K \|\boldsymbol{v}\|_V \|\boldsymbol{w}\|_V, \qquad \forall \boldsymbol{v}, \boldsymbol{w} \in \boldsymbol{\mathcal{D}}_k(\mathcal{E}_h),$$

where κ and K are independent of $\boldsymbol{v}$ and $\boldsymbol{w}$.

Proof. The proof follows the same arguments in [16, Theorems 4.5 and 4.6]. For example, the use of (2.8) and (2.9) leads us to show the coercivity and the continuity. For details, please see [16]. □

Remark 2.3. *Due to the use of inverse polynomial trace inequality, the DG bilinear form will not be coercive and continuous on the broken Sobolev space. In other words,* Theorem 2.1 *holds only on the finite element space. For the choice of the penalty parameter* α_0, *we refer to* [13, 25]. *For instance, we will take* $\alpha_0 \in [10, 100]$ *in the numerical experiments* Section 6.

DG elliptic projection

The DG elliptic projector, $\boldsymbol{R}$, is defined for $\boldsymbol{u} \in \boldsymbol{H}^s(\mathcal{E}_h)$ and $s > 3/2$ by,

$$\boldsymbol{R} : \boldsymbol{H}^s(\mathcal{E}_h) \mapsto \boldsymbol{\mathcal{D}}_k(\mathcal{E}_h) \text{ such that } a(\boldsymbol{u}, \boldsymbol{v}) = a(\boldsymbol{R}\boldsymbol{u}, \boldsymbol{v}), \ \forall \boldsymbol{v} \in \boldsymbol{\mathcal{D}}_k(\mathcal{E}_h).$$

Referring to [20, 21, 14, 25], for example, we recall the following elliptic-error estimates,

$$\left\| \boldsymbol{u} - \boldsymbol{R}\boldsymbol{u} \right\|_V \leqslant C h^{\min(k+1,s)-1} \|\!\|\!\| \boldsymbol{u} \|\!\|\!\|_{H^s(\mathcal{E}_h)}, \tag{2.10}$$

$$\left\| \boldsymbol{u} - \boldsymbol{R}\boldsymbol{u} \right\|_{L_2(\Omega)} \leqslant C h^{\min(k+1,s)} \|\!\|\!\| \boldsymbol{u} \|\!\|\!\|_{H^s(\mathcal{E}_h)}, \tag{2.11}$$

for $\boldsymbol{u} \in \boldsymbol{H}^s(\mathcal{E}_h)$ with $s > 3/2$ and for sufficiently large penalty parameters α_0 and $\beta_0 \geqslant (d-1)^{-1}$. Here, the positive constant C is independent of $\boldsymbol{u}$ but dependent on the domain, its boundary, and the polynomial degree k.

We now move on to describe the model problem.

3 Model Problem

We recall our primal equations (1.1)-(1.6) and hereafter assume the data terms are bounded and smooth so that $\boldsymbol{f} \in C(0, T; \boldsymbol{L}_2(\Omega))$, $\boldsymbol{g}_N \in C^1(0, T; \boldsymbol{L}_2(\Gamma_N))$, $\boldsymbol{u}_0 \in \boldsymbol{H}^s(\Omega)$, and $\boldsymbol{w}_0 \in \boldsymbol{L}_2(\Omega)$. We first of all set up the internal variable representations of viscoelasticity and then give the variational formulations.

3.1 Internal Variables

Recalling the constitutive equation (1.5) and the stress relaxation function (1.6) we define internal variables as

$$\boldsymbol{\psi}_q(t) = \int_0^t \frac{\varphi_q}{\tau_q} e^{-(t-t')/\tau_q} \boldsymbol{u}(t') \, dt' \qquad \text{and} \qquad \boldsymbol{\zeta}_q(t) = \int_0^t \varphi_q e^{-(t-t')/\tau_q} \dot{\boldsymbol{u}}(t') \, dt' \tag{3.1}$$

for $q = 1, \ldots, N_\varphi$, and note that these are zero at $t = 0$. Using (1.6) in (1.5), and the Leibniz integral rule leads us to two alternative forms of the constitutive equation,

$$\underline{\boldsymbol{\sigma}}(\boldsymbol{u}(t)) = \underline{\boldsymbol{D}}\underline{\boldsymbol{\varepsilon}}\left(\varphi_0 \boldsymbol{u}(t) + \sum_{q=1}^{N_\varphi} \boldsymbol{\zeta}_q(t) \right) + \sum_{q=1}^{N_\varphi} \varphi_q e^{-t/\tau_q} \underline{\boldsymbol{D}}\underline{\boldsymbol{\varepsilon}}(\boldsymbol{u}_0), \tag{3.2}$$

$$\text{or} \qquad \underline{\boldsymbol{\sigma}}(\boldsymbol{u}(t)) = \underline{\boldsymbol{D}}\underline{\boldsymbol{\varepsilon}}\left(\boldsymbol{u}(t) - \sum_{q=1}^{N_\varphi} \boldsymbol{\psi}_q(t) \right), \tag{3.3}$$

where we noted that $\boldsymbol{\zeta}_q(t) + \varphi_q e^{-t/\tau_q} \boldsymbol{u}(0) = \varphi_q \boldsymbol{u}(t) - \boldsymbol{\psi}_q(t)$. We call $\boldsymbol{\psi}_q$ (resp. $\boldsymbol{\zeta}_q$) the *displacement form* (resp. *velocity form*) of the internal variable. It is easy to check that (3.3) and (3.2) are equivalent by integration by parts and remembering that $\sum_{q=1}^{N_\varphi} \varphi_q = 1 - \varphi_0$. Using these constitutive relationships we can derive dynamic linear viscoelasticity model problems in two forms as follows.

Displacement form

We consider (1.1) in the form: find $\boldsymbol{u}$, $\boldsymbol{\psi}_1$, $\boldsymbol{\psi}_2$, ..., such that

$$\rho\ddot{\boldsymbol{u}} - \nabla \cdot \underline{\boldsymbol{D}}\underline{\boldsymbol{\varepsilon}}\left(\boldsymbol{u} - \sum_{q=1}^{N_\varphi} \boldsymbol{\psi}_q\right) = \boldsymbol{f}, \tag{3.4}$$

$$\tau_q\dot{\boldsymbol{\psi}}_q + \boldsymbol{\psi}_q = \varphi_q\boldsymbol{u}, \text{ with } \boldsymbol{\psi}(0) = \boldsymbol{0}, \qquad \text{for } q = 1, \ldots, N_\varphi. \tag{3.5}$$

Velocity form

We consider (1.1) in the form:

$$\rho\ddot{\boldsymbol{u}} - \nabla \cdot \underline{\boldsymbol{D}}\underline{\boldsymbol{\varepsilon}}\left(\varphi_0\boldsymbol{u} + \sum_{q=1}^{N_\varphi} \boldsymbol{\zeta}_q\right) = \boldsymbol{f} + \nabla \cdot \left(\sum_{q=1}^{N_\varphi} \varphi_q e^{-t/\tau_q} \underline{\boldsymbol{D}}\underline{\boldsymbol{\varepsilon}}(\boldsymbol{u}_0)\right), \tag{3.6}$$

$$\tau_q\dot{\boldsymbol{\zeta}}_q + \boldsymbol{\zeta}_q = \tau_q\varphi_q\dot{\boldsymbol{u}} \text{ with } \boldsymbol{\zeta}(0) = \boldsymbol{0}, \qquad \text{for } q = 1, \ldots, N_\varphi. \tag{3.7}$$

In these we note that the auxiliary equations (3.5) and (3.7) are derived by time-differentiation of each of (3.1).

Remark 3.1. *The (well known) idea here is to replace the integral form in the constitutive hereditary laws by ODE's for a set of internal variables. With these we use a time stepper rather than numerical integration to compute the discrete solution. Furthermore, while* [22] *employed internal variables as second order tensors, we have defined vector-valued internal variables. This reduces the computer memory requirement by a factor of d.*

3.2 Variational Formulation

We begin by multiplying each of (3.4) and (3.6) by test functions $\boldsymbol{v} \in H^s(\mathcal{E}_h)$, for $s > 3/2$, integrating by parts over each E, summing over every E, and then collecting up terms to form the edge average and jump terms. We then assume sufficient spatial continuity of the continuous solution to (3.4) and (3.7) so that we can add the terms involving the edge jumps of the exact solution: terms three and four on the right of (2.4). This produces the DG bilinear form on the left hand side and gives us a weak form for each choice of the form of the internal variables. The procedure is standard in the DGFEM literature, and for more details in this specific setting we refer to [16] (where it may be useful to note that $\underline{\boldsymbol{\sigma}} \cdot \boldsymbol{n} \cdot \boldsymbol{v} = \underline{\boldsymbol{\sigma}} : (\boldsymbol{v} \otimes \boldsymbol{n})$).

Weak forms

Let us define linear forms by

$$F_d(t; \boldsymbol{v}) = (\boldsymbol{f}(t), \boldsymbol{v}) + (\boldsymbol{g}_N(t), \boldsymbol{v})_{L_2(\Gamma_N)},$$

and

$$F_v(t; \boldsymbol{v}) = (\boldsymbol{f}(t), \boldsymbol{v}) + (\boldsymbol{g}_N(t), \boldsymbol{v})_{L_2(\Gamma_N)} - \sum_{q=1}^{N_\varphi} \varphi_q e^{-t/\tau_q} a(\boldsymbol{u}_0, \boldsymbol{v}).$$

Recalling (2.4), we now use these linear forms to formulate variational problems for the displacement form and the velocity form. First for the displacement form of the problem.

Displacement Form problem, (D) find $\boldsymbol{u}$ and $\{\boldsymbol{\psi}_q\}_{q=1}^{N_\varphi}$ such that for all $\boldsymbol{v} \in \boldsymbol{H}^s(\mathcal{E}_h)$, with $s > 3/2$, we have,

$$(\rho\ddot{\boldsymbol{u}}(t), \boldsymbol{v}) + a(\boldsymbol{u}(t), \boldsymbol{v}) - \sum_{q=1}^{N_\varphi} a(\boldsymbol{\psi}_q(t), \boldsymbol{v}) + J_0^{\alpha_0, \beta_0}(\dot{\boldsymbol{u}}(t), \boldsymbol{v}) = F_d(t; \boldsymbol{v}), \tag{3.8}$$

$$a\left(\tau_q \dot{\boldsymbol{\psi}}_q(t) + \boldsymbol{\psi}_q(t), \boldsymbol{v}\right) = a\left(\varphi_q \boldsymbol{u}(t), \boldsymbol{v}\right), \text{ for each } q, \tag{3.9}$$

where $\boldsymbol{u}(0) = \boldsymbol{u}_0$, $\dot{\boldsymbol{u}}(0) = \boldsymbol{w}_0$ and $\boldsymbol{\psi}_q(0) = \boldsymbol{0}$. And, secondly, for the velocity form.

Velocity Form problem, (V) find $\boldsymbol{u}$ and $\{\boldsymbol{\zeta}_q\}_{q=1}^{N_\varphi}$ such that for all $\boldsymbol{v} \in \boldsymbol{H}^s(\mathcal{E}_h)$, with $s > 3/2$, we have,

$$\left(\rho \ddot{\boldsymbol{u}}(t), \boldsymbol{v}\right) + \varphi_0 a\left(\boldsymbol{u}(t), \boldsymbol{v}\right) + \sum_{q=1}^{N_\varphi} a\left(\boldsymbol{\zeta}_q(t), \boldsymbol{v}\right) + J_0^{\alpha_0, \beta_0}\left(\dot{\boldsymbol{u}}(t), \boldsymbol{v}\right) = F_v(t; \boldsymbol{v}), \tag{3.10}$$

$$a\left(\tau_q \dot{\boldsymbol{\zeta}}_q(t) + \boldsymbol{\zeta}_q(t), \boldsymbol{v}\right) = a\left(\tau_q \varphi_q \dot{\boldsymbol{u}}(t), \boldsymbol{v}\right), \text{ for each } q, \tag{3.11}$$

where $\boldsymbol{u}(0) = \boldsymbol{u}_0$, $\dot{\boldsymbol{u}}(0) = \boldsymbol{w}_0$ and $\boldsymbol{\zeta}_q(0) = \boldsymbol{0}$.

Note that in (3.9) and (3.11) the energy bilinear form, rather than the $L_2(\Omega)$ inner product, is used to enforce the evolution equations for the internal variables. This is because in the testing procedures used below for the stability and error analyses we want to take linear combinations of (3.8) and (3.9), and of (3.10) and (3.11), and their numerical analogues, to cancel certain terms out. We'll return to this in the proof of Theorem 4.1 below.

Fully discrete formulations

For the time discretisation we employ a *Crank-Nicolson* type finite difference scheme [7]. Let $t_n = n\Delta t$ with $\Delta t = T/N$ for some $N \in \mathbb{N}$, and denote the fully discrete approximations to $\boldsymbol{u}$ and $\dot{\boldsymbol{u}}$ by $\boldsymbol{u}(t_n) = \boldsymbol{u}^n \approx \boldsymbol{U}_h^n \in \mathcal{D}_k(\mathcal{E}_h)$ and $\dot{\boldsymbol{u}}(t_n) = \dot{\boldsymbol{u}}^n \approx \boldsymbol{W}_h^n \in \mathcal{D}_k(\mathcal{E}_h)$. Similarly, for the internal variables we introduce $\boldsymbol{\psi}_q(t_n) \approx \boldsymbol{\Psi}_{hq}^n \in \mathcal{D}_k(\mathcal{E}_h)$ and $\boldsymbol{\zeta}_q(t_n) \approx \boldsymbol{\mathcal{S}}_{hq}^n \in \mathcal{D}_k(\mathcal{E}_h)$, for each q. Furthermore, in the schemes that follow we will use the following approximations,

$$\frac{\ddot{\boldsymbol{u}}(t_{n+1}) + \ddot{\boldsymbol{u}}(t_n)}{2} \approx \frac{\boldsymbol{W}_h^{n+1} - \boldsymbol{W}_h^n}{\Delta t} \text{ and } \frac{\boldsymbol{u}(t_{n+1}) + \boldsymbol{u}(t_n)}{2} \approx \frac{\boldsymbol{U}_h^{n+1} + \boldsymbol{U}_h^n}{2},$$

and we will impose the relation,

$$\frac{\boldsymbol{W}_h^{n+1} + \boldsymbol{W}_h^n}{2} = \frac{\boldsymbol{U}_h^{n+1} - \boldsymbol{U}_h^n}{\Delta t}. \tag{3.12}$$

We can now give the fully discrete schemes.

Displacement Form problem, (D)^h find $\boldsymbol{W}_h^n, \boldsymbol{U}_h^n, \boldsymbol{\Psi}_{h1}^n, \ldots, \boldsymbol{\Psi}_{hN_\varphi}^n \in \mathcal{D}_k(\mathcal{E}_h)$ for $n = 0, \ldots, N$ such that for all $\boldsymbol{v} \in \mathcal{D}_k(\mathcal{E}_h)$ we have for $n = 0, 1, \ldots, N-1$ firstly that,

$$\left(\rho \frac{\boldsymbol{W}_h^{n+1} - \boldsymbol{W}_h^n}{\Delta t}, \boldsymbol{v}\right) + a\left(\frac{\boldsymbol{U}_h^{n+1} + \boldsymbol{U}_h^n}{2}, \boldsymbol{v}\right) - \sum_{q=1}^{N_\varphi} a\left(\frac{\boldsymbol{\Psi}_{hq}^{n+1} + \boldsymbol{\Psi}_{hq}^n}{2}, \boldsymbol{v}\right)$$

$$+ J_0^{\alpha_0, \beta_0}\left(\frac{\boldsymbol{W}_h^{n+1} + \boldsymbol{W}_h^n}{2}, \boldsymbol{v}\right) = \frac{1}{2}\left(F_d^{n+1}(\boldsymbol{v}) + F_d^n(\boldsymbol{v})\right), \tag{3.13}$$

and secondly that for $q = 1, 2, \ldots, N_\varphi$,

$$a\left(\tau_q \frac{\boldsymbol{\Psi}_{hq}^{n+1} - \boldsymbol{\Psi}_{hq}^n}{\Delta t} + \frac{\boldsymbol{\Psi}_{hq}^{n+1} + \boldsymbol{\Psi}_{hq}^n}{2}, \boldsymbol{v}\right) = a\left(\varphi_q \frac{\boldsymbol{U}_h^{n+1} + \boldsymbol{U}_h^n}{2}, \boldsymbol{v}\right), \tag{3.14}$$

with initial data

$$a\left(\boldsymbol{U}_h^0, \boldsymbol{v}\right) = a\left(\boldsymbol{u}_0, \boldsymbol{v}\right), \tag{3.15}$$

$$\left(\boldsymbol{W}_h^0, \boldsymbol{v}\right) = \left(\boldsymbol{w}_0, \boldsymbol{v}\right), \tag{3.16}$$

$$\boldsymbol{\Psi}_{hq}^0 = \boldsymbol{0}, \ \forall q = 1, \ldots, N_\varphi, \tag{3.17}$$

and where $F_d^n(\boldsymbol{v}) = F_d(t_n; \boldsymbol{v})$.

Velocity Form problem, $(\mathbf{V})^h$ find $\boldsymbol{W}_h^n$, $\boldsymbol{U}_h^n$, $\boldsymbol{\mathcal{S}}_{h1}^n, \ldots, \boldsymbol{\mathcal{S}}_{hN_\varphi}^n \in \boldsymbol{\mathcal{D}}_k(\mathcal{E}_h)$ for $n = 0, \ldots, N$ such that for all $\boldsymbol{v} \in \boldsymbol{\mathcal{D}}_k(\mathcal{E}_h)$ we have for $n = 0, 1, \ldots, N-1$ firstly that,

$$
\left(\rho \frac{\boldsymbol{W}_h^{n+1} - \boldsymbol{W}_h^n}{\Delta t}, \boldsymbol{v} \right) + \varphi_0 a \left(\frac{\boldsymbol{U}_h^{n+1} + \boldsymbol{U}_h^n}{2}, \boldsymbol{v} \right) + \sum_{q=1}^{N_\varphi} a \left(\frac{\boldsymbol{\mathcal{S}}_{hq}^{n+1} + \boldsymbol{\mathcal{S}}_{hq}^n}{2}, \boldsymbol{v} \right)
$$

$$
+ J_0^{\alpha_0, \beta_0} \left(\frac{\boldsymbol{W}_h^{n+1} + \boldsymbol{W}_h^n}{2}, \boldsymbol{v} \right) = \frac{1}{2} \left(F_v^{n+1}(\boldsymbol{v}) + F_v^n(\boldsymbol{v}) \right), \tag{3.18}
$$

and secondly that for $q = 1, 2, \ldots, N_\varphi$,

$$
a \left(\tau_q \frac{\boldsymbol{\mathcal{S}}_{hq}^{n+1} - \boldsymbol{\mathcal{S}}_{hq}^n}{\Delta t} + \frac{\boldsymbol{\mathcal{S}}_{hq}^{n+1} + \boldsymbol{\mathcal{S}}_{hq}^n}{2}, \boldsymbol{v} \right) = a \left(\tau_q \varphi_q \frac{\boldsymbol{W}_h^{n+1} + \boldsymbol{W}_h^n}{2}, \boldsymbol{v} \right), \tag{3.19}
$$

with initial data (3.15), (3.16),

$$
\boldsymbol{\mathcal{S}}_{hq}^0 = \boldsymbol{0}, \ \forall q = 1, \ldots, N_\varphi, \tag{3.20}
$$

and where $F_v^n(\boldsymbol{v}) = F_v(t_n; \boldsymbol{v})$.

The jump term penalization of the velocities in (3.8) and (3.10) is included in these formulations to facilitate the error analysis later: see (5.10) in particular. This term is not required for the stability estimates that follow.

4 Stability Analysis

In this section we derive stability bounds for the solutions to the fully discrete displacement and velocity forms of the problem. As the problems are linear, these stability bounds can also be used to conclude the existence and uniqueness of the numerical solutions and, hence, the well-posedness of the discrete problems. At first we present bounds that are non-optimal in that they contain a factor of $h^{-1} \|\boldsymbol{g}_N\|_{H^1(0,T;L_2(\Gamma_N))}^2$ on the right hand side. This arises from use of the trace inequality on the traction term. This unwelcome appearance of h^{-1} is not unusual (see for example [20, 22]), and is a technical issue stemming from the straightforward use of (4.3) below.

The h^{-1} factor is not observed in practical computations, suggesting that it can be removed. This can be seen by using the deeper and non-trivial arguments given by Buffa and Ortner in [5]. There, under some quite mild mesh assumptions, the trace bound follows without the factor of h^{-1} appearing. We give more details on this below the non-optimal results that follow, and there we set the improved results forward as a corollary.

Theorem 4.1 (Stability bound for $(\mathbf{D})^h$). *If $\beta_0(d-1) \geqslant 1$ and α_0 is large enough, and if $\boldsymbol{W}_h^n$, $\boldsymbol{U}_h^n$ and $\{\boldsymbol{\Psi}_{hq}^n\}_{q=1}^{N_\varphi}$ in $\boldsymbol{\mathcal{D}}_k(\mathcal{E}_h)$ satisfy the fully discrete formulation $(\mathbf{D})^h$, then there exists a positive constant C such that*

$$
\max_{0 \leqslant n \leqslant N} \|\boldsymbol{W}_h^n\|_{L_2(\Omega)}^2 + \max_{0 \leqslant n \leqslant N} \|\boldsymbol{U}_h^n\|_V^2 + \sum_{q=1}^{N_\varphi} \max_{0 \leqslant n \leqslant N} \|\boldsymbol{\Psi}_{hq}^n\|_V^2 + \sum_{n=0}^{N-1} \sum_{q=1}^{N_\varphi} \frac{1}{\Delta t} \|\boldsymbol{\Psi}_{hq}^{n+1} - \boldsymbol{\Psi}_{hq}^n\|_V^2
$$

$$
+ \Delta t \sum_{n=0}^{N-1} J_0^{\alpha_0, \beta_0} \left(\boldsymbol{W}_h^{n+1} + \boldsymbol{W}_h^n, \boldsymbol{W}_h^{n+1} + \boldsymbol{W}_h^n \right)
$$

$$
\leqslant C T^2 \left(\|\boldsymbol{w}_0\|_{L_2(\Omega)}^2 + \|\boldsymbol{u}_0\|_V^2 + \|\boldsymbol{f}\|_{L_\infty(0,T;L_2(\Omega))}^2 + h^{-1} \|\boldsymbol{g}_N\|_{H^1(0,T;L_2(\Gamma_N))}^2 \right).
$$

Here, C is independent of the discrete solutions, Δt, and h, but dependent on the polynomial degree k, the domain Ω, its boundary, and the material properties.

Proof. Choose $m \in \mathbb{N}$ so that $m < N$. Take $\boldsymbol{v} = \Delta t(\boldsymbol{W}_h^{n+1} + \boldsymbol{W}_h^n)$ in (3.13) and $\boldsymbol{v} = 2(\boldsymbol{\Psi}_{hq}^{n+1} - \boldsymbol{\Psi}_{hq}^n)$ in (3.14), for each q, and for $n = 0, \ldots, m-1$, and then add the results and sum over n to get,

$$
\rho\big\|\boldsymbol{W}_h^m\big\|_{L_2(\Omega)}^2 + a\left(\boldsymbol{U}_h^m, \boldsymbol{U}_h^m\right) + \sum_{q=1}^{N_\varphi} \frac{1}{\varphi_q} a\left(\boldsymbol{\Psi}_{hq}^m, \boldsymbol{\Psi}_{hq}^m\right) + \sum_{n=0}^{m-1} \sum_{q=1}^{N_\varphi} \frac{2\tau_q}{\Delta t \varphi_q} a\left(\boldsymbol{\Psi}_{hq}^{n+1} - \boldsymbol{\Psi}_{hq}^n, \boldsymbol{\Psi}_{hq}^{n+1} - \boldsymbol{\Psi}_{hq}^n\right)
$$

$$
+ \frac{\Delta t}{2} \sum_{n=0}^{m-1} J_0^{\alpha_0,\beta_0}\left(\boldsymbol{W}_h^{n+1} + \boldsymbol{W}_h^n, \boldsymbol{W}_h^{n+1} + \boldsymbol{W}_h^n\right)
$$

$$
= \rho\big\|\boldsymbol{W}_h^0\big\|_{L_2(\Omega)}^2 + a\left(\boldsymbol{U}_h^0, \boldsymbol{U}_h^0\right) + 2\sum_{q=1}^{N_\varphi} a\left(\boldsymbol{\Psi}_{hq}^m, \boldsymbol{U}_h^m\right)
$$

$$
+ \frac{\Delta t}{2} \sum_{n=0}^{m-1} \left(F_d^{n+1}(\boldsymbol{W}_h^{n+1} + \boldsymbol{W}_h^n) + F_d^n(\boldsymbol{W}_h^{n+1} + \boldsymbol{W}_h^n)\right) \tag{4.1}
$$

since, by (3.12), $\Delta t(\boldsymbol{W}_h^{n+1} + \boldsymbol{W}_h^n) = 2(\boldsymbol{U}_h^{n+1} - \boldsymbol{U}_h^n)$ and, by (3.17), $\boldsymbol{\Psi}_{hq}^0 = \boldsymbol{0}$, and also where we noted that

$$
a\left(\boldsymbol{\Psi}_{hq}^{n+1} + \boldsymbol{\Psi}_{hq}^n, \boldsymbol{U}_h^{n+1} - \boldsymbol{U}_h^n\right) = 2a\left(\boldsymbol{\Psi}_{hq}^{n+1}, \boldsymbol{U}_h^{n+1}\right) - 2a\left(\boldsymbol{\Psi}_{hq}^n, \boldsymbol{U}_h^n\right) - a\left(\boldsymbol{\Psi}_{hq}^{n+1} - \boldsymbol{\Psi}_{hq}^n, \boldsymbol{U}_h^{n+1} + \boldsymbol{U}_h^n\right)
$$

which, when used with (3.14), gives us,

$$
a\left(\boldsymbol{\Psi}_{hq}^{n+1} + \boldsymbol{\Psi}_{hq}^n, \boldsymbol{U}_h^{n+1} - \boldsymbol{U}_h^n\right) = 2a\left(\boldsymbol{\Psi}_{hq}^{n+1}, \boldsymbol{U}_h^{n+1}\right) - 2a\left(\boldsymbol{\Psi}_{hq}^n, \boldsymbol{U}_h^n\right)
$$

$$
- \frac{2\tau_q}{\Delta t \, \varphi_q} a\left(\boldsymbol{\Psi}_{hq}^{n+1} - \boldsymbol{\Psi}_{hq}^n, \boldsymbol{\Psi}_{hq}^{n+1} - \boldsymbol{\Psi}_{hq}^n\right) - \frac{1}{\varphi_q}\left(a\left(\boldsymbol{\Psi}_{hq}^{n+1}, \boldsymbol{\Psi}_{hq}^{n+1}\right) - a\left(\boldsymbol{\Psi}_{hq}^n, \boldsymbol{\Psi}_{hq}^n\right)\right)
$$

for each n and q. The cancellation of terms in this step illustrates the importance of enforcing the internal variable ODE's in the energy bilinear form in (3.9) and (3.11). Using (2.6), (4.1) and Theorem 2.1 in (4.1) we obtain,

$$
\rho\big\|\boldsymbol{W}_h^m\big\|_{L_2(\Omega)}^2 + \big\|\boldsymbol{U}_h^m\big\|_V^2 + \sum_{q=1}^{N_\varphi} \frac{1}{\varphi_q} \big\|\boldsymbol{\Psi}_{hq}^m\big\|_V^2 + \sum_{n=0}^{m-1} \sum_{q=1}^{N_\varphi} \frac{2\kappa\tau_q}{\Delta t \varphi_q} \big\|\boldsymbol{\Psi}_{hq}^{n+1} - \boldsymbol{\Psi}_{hq}^n\big\|_V^2
$$

$$
+ \frac{\Delta t}{2} \sum_{n=0}^{m-1} J_0^{\alpha_0,\beta_0}\left(\boldsymbol{W}_h^{n+1} + \boldsymbol{W}_h^n, \boldsymbol{W}_h^{n+1} + \boldsymbol{W}_h^n\right)
$$

$$
\leqslant \bigg| \rho\big\|\boldsymbol{W}_h^0\big\|_{L_2(\Omega)}^2 + a\left(\boldsymbol{U}_h^0, \boldsymbol{U}_h^0\right) + 2\sum_{q=1}^{N_\varphi} a\left(\boldsymbol{\Psi}_{hq}^m, \boldsymbol{U}_h^m\right)
$$

$$
+ \frac{\Delta t}{2} \sum_{n=0}^{m-1} \left(F_d^{n+1}(\boldsymbol{W}_h^{n+1} + \boldsymbol{W}_h^n) + F_d^n(\boldsymbol{W}_h^{n+1} + \boldsymbol{W}_h^n)\right)
$$

$$
+ 2\sum_{e \subset \Gamma_h \cup \Gamma_D} \int_e \{\underline{\boldsymbol{D}}\boldsymbol{\varepsilon}(\boldsymbol{U}_h^m)\} : [\boldsymbol{U}_h^m \otimes \boldsymbol{n}_e]de + \sum_{q=1}^{N_\varphi} \frac{2}{\varphi_q} \sum_{e \subset \Gamma_h \cup \Gamma_D} \int_e \{\underline{\boldsymbol{D}}\boldsymbol{\varepsilon}(\boldsymbol{\Psi}_{hq}^m)\} : [\boldsymbol{\Psi}_{hq}^m \otimes \boldsymbol{n}_e]de \bigg|. \tag{4.2}
$$

Now we show an upper bound for the right hand side of (4.2).

- $\big\|\boldsymbol{W}_h^0\big\|_{L_2(\Omega)}^2$: By the Cauchy-Schwarz inequality, (3.16) yields

$$
\big\|\boldsymbol{W}_h^0\big\|_{L_2(\Omega)}^2 = \left(\boldsymbol{W}_h^0, \boldsymbol{W}_h^0\right) = \left(\boldsymbol{W}_h^0, \boldsymbol{w}_0\right) \leqslant \big\|\boldsymbol{W}_h^0\big\|_{L_2(\Omega)} \big\|\boldsymbol{w}_0\big\|_{L_2(\Omega)},
$$

hence $\big\|\boldsymbol{W}_h^0\big\|_{L_2(\Omega)}^2 \leqslant \big\|\boldsymbol{w}_0\big\|_{L_2(\Omega)}^2$.

- $\big|a\left(\boldsymbol{U}_h^0, \boldsymbol{U}_h^0\right)\big|$: Combining the coercivity and the continuity, we can derive

$$
\kappa\big\|\boldsymbol{U}_h^0\big\|_V^2 \leqslant a\left(\boldsymbol{U}_h^0, \boldsymbol{U}_h^0\right) = a\left(\boldsymbol{U}_h^0, \boldsymbol{u}_0\right) \leqslant K\big\|\boldsymbol{U}_h^0\big\|_V \big\|\boldsymbol{u}_0\big\|_V,
$$

by (3.15). This implies $\left\|\boldsymbol{U}_h^0\right\|_V \leqslant K/\kappa \left\|\boldsymbol{u}_0\right\|_V$ and so we have

$$\left| a\left(\boldsymbol{U}_h^0, \boldsymbol{U}_h^0\right) \right| \leqslant K\left\|\boldsymbol{U}_h^0\right\|_V^2 \leqslant \bar{K}\left\|\boldsymbol{u}_0\right\|_V^2 \qquad \text{for } \bar{K} = \frac{K^3}{\kappa^2}.$$

- $\left| 2\sum_{q=1}^{N_\varphi} a\left(\boldsymbol{\Psi}_{hq}^m, \boldsymbol{U}_h^m\right) \right|$: The Cauchy-Schwarz inequality, Young's inequality and (2.9) yield

$$\left| 2\sum_{q=1}^{N_\varphi} a\left(\boldsymbol{\Psi}_{hq}^m, \boldsymbol{U}_h^m\right) \right| \leqslant \sum_{q=1}^{N_\varphi}\left(\epsilon_q + \frac{C}{\sqrt{\alpha_0}}\right)\left\|\boldsymbol{U}_h^m\right\|_V^2 + \sum_{q=1}^{N_\varphi}\left(\frac{1}{\epsilon_q} + \frac{C}{\sqrt{\alpha_0}}\right)\left\|\boldsymbol{\Psi}_{hq}^m\right\|_V^2,$$

for any positive ϵ_q, $\forall q$.

- $\left| \frac{\Delta t}{2}\sum_{n=0}^{m-1}\left(F_d^{n+1}(\boldsymbol{W}_h^{n+1} + \boldsymbol{W}_h^n) + F_d^n(\boldsymbol{W}_h^{n+1} + \boldsymbol{W}_h^n)\right) \right|$: Note that summation by parts and the fundamental theorem of calculus give

$$\sum_{n=0}^{m-1}\left(\boldsymbol{g}_N(t_{n+1}) + \boldsymbol{g}_N(t_n), \boldsymbol{U}_h^{n+1} - \boldsymbol{U}_h^n\right)_{L_2(e)} = 2\left(\boldsymbol{g}_N(t_m), \boldsymbol{U}_h^m\right)_{L_2(e)} - 2\left(\boldsymbol{g}_N(t_0), \boldsymbol{U}_h^0\right)_{L_2(e)}$$
$$- \sum_{n=0}^{m-1}\int_{t_n}^{t_{n+1}}\left(\dot{\boldsymbol{g}}_N(t'), \boldsymbol{U}_h^{n+1} + \boldsymbol{U}_h^n\right)_{L_2(e)}dt', \qquad \forall e \subset \Gamma_N.$$

By (3.12) and the Cauchy-Schwarz inequality, we therefore have

$$\left| \frac{\Delta t}{2}\sum_{n=0}^{m-1}\left(F_d^{n+1}(\boldsymbol{W}_h^{n+1} + \boldsymbol{W}_h^n) + F_d^n(\boldsymbol{W}_h^{n+1} + \boldsymbol{W}_h^n)\right) \right|$$
$$\leqslant \frac{\Delta t}{2}\sum_{n=0}^{m-1}\left(\left\|\boldsymbol{f}^{n+1}\right\|_{L_2(\Omega)} + \left\|\boldsymbol{f}^n\right\|_{L_2(\Omega)}\right)\left\|\boldsymbol{W}_h^{n+1} + \boldsymbol{W}_h^n\right\|_{L_2(\Omega)}$$
$$+ 2\sum_{e\subset\Gamma_N}\left\|\boldsymbol{g}_N^m\right\|_{L_2(e)}\left\|\boldsymbol{U}_h^m\right\|_{L_2(e)} + 2\sum_{e\subset\Gamma_N}\left\|\boldsymbol{g}_N^0\right\|_{L_2(e)}\left\|\boldsymbol{U}_h^0\right\|_{L_2(e)}$$
$$+ \sum_{n=0}^{m-1}\int_{t_n}^{t_{n+1}}\sum_{e\subset\Gamma_N}\left\|\dot{\boldsymbol{g}}_N(t')\right\|_{L_2(e)}\left\|\boldsymbol{U}_h^{n+1} + \boldsymbol{U}_h^n\right\|_{L_2(e)}dt'.$$

Since the inverse polynomial trace and Poincaré's inequalities, (2.1) and (2.2), imply that

$$\sum_{e\subset\partial\Omega}\|\boldsymbol{v}\|_{L_2(e)}^2 \leqslant Ch^{-1}\sum_{E\in\mathcal{E}_h}\|\boldsymbol{v}\|_{L_2(E)}^2 \leqslant Ch^{-1}\|\boldsymbol{v}\|_V^2 \qquad \forall\boldsymbol{v}\in\boldsymbol{\mathcal{D}}_k(\mathcal{E}_h), \tag{4.3}$$

the triangle and Young's inequalities lead us to,

$$\left| \frac{\Delta t}{2}\sum_{n=0}^{m-1}\left(F_d^{n+1}(\boldsymbol{W}_h^{n+1} + \boldsymbol{W}_h^n) + F_d^n(\boldsymbol{W}_h^{n+1} + \boldsymbol{W}_h^n)\right) \right|$$
$$\leqslant \frac{\Delta t}{4\epsilon_a}\sum_{n=0}^{m-1}\left(\left\|\boldsymbol{f}^{n+1}\right\|_{L_2(\Omega)}^2 + \left\|\boldsymbol{f}^n\right\|_{L_2(\Omega)}^2\right) + 2\Delta t\epsilon_a\sum_{n=0}^{m-1}\left(\left\|\boldsymbol{W}_h^{n+1}\right\|_{L_2(\Omega)}^2 + \left\|\boldsymbol{W}_h^n\right\|_{L_2(\Omega)}^2\right)$$
$$+ \frac{1}{\epsilon_b}\left\|\boldsymbol{g}_N^m\right\|_{L_2(\Gamma_N)}^2 + \frac{C\epsilon_b}{h}\left\|\boldsymbol{U}_h^m\right\|_V^2 + \frac{1}{\epsilon_b}\left\|\boldsymbol{g}_N^0\right\|_{L_2(\Gamma_N)}^2 + C\left\|\boldsymbol{U}_h^0\right\|_V^2$$
$$+ \frac{1}{\epsilon_b}\int_0^{t_m}\left\|\dot{\boldsymbol{g}}_N(t')\right\|_{L_2(\Gamma_N)}^2 dt' + \frac{C\Delta t\epsilon_b}{2h}\sum_{n=0}^{m-1}\left(\left\|\boldsymbol{U}_h^{n+1}\right\|_V^2 + \left\|\boldsymbol{U}_h^n\right\|_V^2\right),$$

for any positive ϵ_a and ϵ_b. Maximizing over time we then arrive at,

$$
\left| \frac{\Delta t}{2} \sum_{n=0}^{m-1} \left(F_d^{n+1}(\boldsymbol{W}_h^{n+1} + \boldsymbol{W}_h^n) + F_d^n(\boldsymbol{W}_h^{n+1} + \boldsymbol{W}_h^n) \right) \right|
$$

$$
\leqslant \frac{T}{2\epsilon_a} \|\boldsymbol{f}\|_{L_\infty(0,T;L_2(\Omega))}^2 + 4T\epsilon_a \max_{0\leqslant n\leqslant N} \|\boldsymbol{W}_h^n\|_{L_2(\Omega)}^2 + \left(\frac{1}{\epsilon_b} + \frac{1}{h} \right) \|\boldsymbol{g}_N\|_{L_\infty(0,T;L_2(\Gamma_N))}^2
$$

$$
+ C\|\boldsymbol{U}_h^0\|_V^2 + \frac{1}{\epsilon_b} \|\dot{\boldsymbol{g}}_N\|_{L_2(0,T;L_2(\Gamma_N))}^2 + \frac{C(T+1)\epsilon_b}{h} \max_{0\leqslant n\leqslant N} \|\boldsymbol{U}_h^n\|_V^2.
$$

- $\left| 2 \sum_{e\subset\Gamma_h\cup\Gamma_D} \int_e \{\underline{\boldsymbol{D}}\underline{\varepsilon}(\boldsymbol{U}_h^m)\} : [\boldsymbol{U}_h^m \otimes \boldsymbol{n}_e] de \right|$: (2.9) implies that

$$
\left| 2 \sum_{e\subset\Gamma_h\cup\Gamma_D} \int_e \{\underline{\boldsymbol{D}}\underline{\varepsilon}(\boldsymbol{U}_h^m)\} : [\boldsymbol{U}_h^m \otimes \boldsymbol{n}_e] de \right| \leqslant \frac{C}{\sqrt{\alpha_0}} \|\boldsymbol{U}_h^m\|_V^2.
$$

- $\left| \sum_{q=1}^{N_\varphi} \frac{2}{\varphi_q} \sum_{e\subset\Gamma_h\cup\Gamma_D} \int_e \{\underline{\boldsymbol{D}}\underline{\varepsilon}(\boldsymbol{\Psi}_{hq}^m)\} : [\boldsymbol{\Psi}_{hq}^m \otimes \boldsymbol{n}_e] de \right|$: In the same manner, (2.9) yields

$$
\left| \sum_{q=1}^{N_\varphi} \frac{2}{\varphi_q} \sum_{e\subset\Gamma_h\cup\Gamma_D} \int_e \{\underline{\boldsymbol{D}}\underline{\varepsilon}(\boldsymbol{\Psi}_{hq}^m)\} : [\boldsymbol{\Psi}_{hq}^m \otimes \boldsymbol{n}_e] de \right| \leqslant \sum_{q=1}^{N_\varphi} \frac{C}{\varphi_q\sqrt{\alpha_0}} \|\boldsymbol{\Psi}_{hq}^m\|_V^2.
$$

Collecting these results together then gives,

$$
\rho\|\boldsymbol{W}_h^m\|_{L_2(\Omega)}^2 + \left(1 - \sum_{q=1}^{N_\varphi} \epsilon_q - \frac{CN_\varphi}{\sqrt{\alpha_0}} \right) \|\boldsymbol{U}_h^m\|_V^2
$$

$$
+ \sum_{q=1}^{N_\varphi} \left(\frac{1}{\varphi_q} - \frac{1}{\epsilon_q} - \frac{C}{\sqrt{\alpha_0}} \right) \|\boldsymbol{\Psi}_{hq}^m\|_V^2 + \sum_{n=0}^{m-1} \sum_{q=1}^{N_\varphi} \frac{2\kappa\tau_q}{\Delta t\varphi_q} \|\boldsymbol{\Psi}_{hq}^{n+1} - \boldsymbol{\Psi}_{hq}^n\|_V^2
$$

$$
+ \frac{\Delta t}{2} \sum_{n=0}^{m-1} J_0^{\alpha_0,\beta_0} \left(\boldsymbol{W}_h^{n+1} + \boldsymbol{W}_h^n, \boldsymbol{W}_h^{n+1} + \boldsymbol{W}_h^n \right)
$$

$$
\leqslant \rho\|\boldsymbol{w}_0\|_{L_2(\Omega)}^2 + (\bar{K} + CK/\kappa)\|\boldsymbol{u}_0\|_V^2 + \frac{T}{2\epsilon_a} \|\boldsymbol{f}\|_{L_\infty(0,T;L_2(\Omega))}^2
$$

$$
+ \left(\frac{1}{\epsilon_b} + \frac{1}{h} \right) \|\boldsymbol{g}_N\|_{L_\infty(0,T;L_2(\Gamma_N))}^2 + \frac{1}{\epsilon_b} \|\dot{\boldsymbol{g}}_N\|_{L_2(0,T;L_2(\Gamma_N))}^2
$$

$$
+ 4T\epsilon_a \max_{0\leqslant n\leqslant N} \|\boldsymbol{W}_h^n\|_{L_2(\Omega)}^2 + \frac{C(T+1)\epsilon_b}{h} \max_{0\leqslant n\leqslant N} \|\boldsymbol{U}_h^n\|_V^2. \tag{4.4}
$$

When we set $\epsilon_q = \varphi_q + \varphi_0/(2N_\varphi) > 0$ for each q, and use (1.7) to obtain,

$$
1 - \sum_{q=1}^{N_\varphi} \epsilon_q = 1 - \sum_{q=1}^{N_\varphi} \varphi_q - \sum_{q=1}^{N_\varphi} \frac{\varphi_0}{2N_\varphi} = \varphi_0 - \frac{\varphi_0}{2} = \frac{\varphi_0}{2} > 0,
$$

(4.4) gives

$$
\rho\|\boldsymbol{W}_h^m\|_{L_2(\Omega)}^2 + \left(\frac{\varphi_0}{2} - \frac{CN_\varphi}{\sqrt{\alpha_0}} \right) \|\boldsymbol{U}_h^m\|_V^2
$$

$$
+ \sum_{q=1}^{N_\varphi} \left(\frac{\varphi_0}{2N_\varphi\varphi_q^2 + \varphi_0\varphi_q} - \frac{C}{\sqrt{\alpha_0}} \right) \|\boldsymbol{\Psi}_{hq}^m\|_V^2 + \sum_{n=0}^{m-1} \sum_{q=1}^{N_\varphi} \frac{2\kappa\tau_q}{\Delta t\varphi_q} \|\boldsymbol{\Psi}_{hq}^{n+1} - \boldsymbol{\Psi}_{hq}^n\|_V^2
$$

$$+\frac{\Delta t}{2}\sum_{n=0}^{m-1}J_0^{\alpha_0,\beta_0}\left(\boldsymbol{W}_h^{n+1}+\boldsymbol{W}_h^n,\boldsymbol{W}_h^{n+1}+\boldsymbol{W}_h^n\right)$$

$$\leqslant\rho\left\|\boldsymbol{w}_0\right\|_{L_2(\Omega)}^2+(\bar{K}+CK/\kappa)\left\|\boldsymbol{u}_0\right\|_V^2+\frac{T}{2\epsilon_a}\left\|\boldsymbol{f}\right\|_{L_\infty(0,T;L_2(\Omega))}^2$$

$$+\left(\frac{1}{\epsilon_b}+\frac{1}{h}\right)\left\|\boldsymbol{g}_N\right\|_{L_\infty(0,T;L_2(\Gamma_N))}^2+\frac{1}{\epsilon_b}\left\|\dot{\boldsymbol{g}}_N\right\|_{L_2(0,T;L_2(\Gamma_N))}^2$$

$$+4T\epsilon_a\max_{0\leqslant n\leqslant N}\left\|\boldsymbol{W}_h^n\right\|_{L_2(\Omega)}^2+\frac{C(T+1)\epsilon_b}{h}\max_{0\leqslant n\leqslant N}\left\|\boldsymbol{U}_h^n\right\|_V^2.\tag{4.5}$$

After noting that the right hand side of (4.5) is independent of m, and that m is arbitrary, we can obtain

$$\frac{\rho}{2}\max_{0\leqslant n\leqslant N}\left\|\boldsymbol{W}_h^n\right\|_{L_2(\Omega)}^2+\left(\frac{\varphi_0}{4}-\frac{CN_\varphi}{\sqrt{\alpha_0}}\right)\max_{0\leqslant n\leqslant N}\left\|\boldsymbol{U}_h^n\right\|_V^2+\sum_{q=1}^{N_\varphi}\left(\frac{\varphi_0}{2N_\varphi\varphi_q^2+\varphi_0\varphi_q}-\frac{C}{\sqrt{\alpha_0}}\right)\max_{0\leqslant n\leqslant N}\left\|\boldsymbol{\Psi}_{hq}^n\right\|_V^2$$

$$+\sum_{n=0}^{N-1}\sum_{q=1}^{N_\varphi}\frac{2\kappa\tau_q}{\Delta t\varphi_q}\left\|\boldsymbol{\Psi}_{hq}^{n+1}-\boldsymbol{\Psi}_{hq}^n\right\|_V^2+\frac{\Delta t}{2}\sum_{n=0}^{N-1}J_0^{\alpha_0,\beta_0}\left(\boldsymbol{W}_h^{n+1}+\boldsymbol{W}_h^n,\boldsymbol{W}_h^{n+1}+\boldsymbol{W}_h^n\right)$$

$$\leqslant\rho\left\|\boldsymbol{w}_0\right\|_{L_2(\Omega)}^2+(\bar{K}+CK/\kappa)\left\|\boldsymbol{u}_0\right\|_V^2+\frac{4T^2}{\rho}\left\|\boldsymbol{f}\right\|_{L_\infty(0,T;L_2(\Omega))}^2$$

$$+\frac{1}{h}\left(\frac{4C(T+1)}{\varphi_0}+1\right)\left\|\boldsymbol{g}_N\right\|_{L_\infty(0,T;L_2(\Gamma_N))}^2+\frac{4C(T+1)}{\varphi_0 h}\left\|\dot{\boldsymbol{g}}_N\right\|_{L_2(0,T;L_2(\Gamma_N))}^2,\tag{4.6}$$

where $\epsilon_a=\rho/(8T)$ and $\epsilon_b=\varphi_0 h/(4C(T+1))$. Taking α_0 sufficiently large then completes the proof. □

Theorem 4.2 (Stability bound for $(\mathbf{V})^h$). *If $\beta_0(d-1)\geqslant 1$ and α_0 is large enough, and if $\boldsymbol{W}_h^n$, $\boldsymbol{U}_h^n$ and $\{\boldsymbol{S}_{hq}^n\}_{q=1}^{N_\varphi}$ satisfy the fully discrete formulation $(\mathbf{V})^h$, then there exists a positive constant C such that*

$$\max_{0\leqslant n\leqslant N}\left\|\boldsymbol{W}_h^n\right\|_{L_2(\Omega)}^2+\max_{0\leqslant n\leqslant N}\left\|\boldsymbol{S}_h^n\right\|_V^2+\sum_{q=1}^{N_\varphi}\max_{0\leqslant n\leqslant N}\left\|\boldsymbol{\Psi}_{hq}^n\right\|_V^2+\sum_{n=0}^{N-1}\sum_{q=1}^{N_\varphi}\Delta t\left\|\boldsymbol{S}_{hq}^{n+1}-\boldsymbol{S}_{hq}^n\right\|_V^2$$

$$+\Delta t\sum_{n=0}^{N-1}J_0^{\alpha_0,\beta_0}\left(\boldsymbol{W}_h^{n+1}+\boldsymbol{W}_h^n,\boldsymbol{W}_h^{n+1}+\boldsymbol{W}_h^n\right)$$

$$\leqslant CT^2\left(\left\|\boldsymbol{w}_0\right\|_{L_2(\Omega)}^2+\left\|\boldsymbol{u}_0\right\|_V^2+\left\|\boldsymbol{f}\right\|_{L_\infty(0,T;L_2(\Omega))}^2+h^{-1}\left\|\boldsymbol{g}_N\right\|_{H^1(0,T;L_2(\Gamma_N))}^2\right).$$

Here, C is independent of discrete solutions, Δt and h but dependent on the polynomial degree k, the domain Ω, its boundary, and the material properties.

Proof. The proof follows the same arguments in Theorem 4.1. We take $\boldsymbol{v}=\Delta t(\boldsymbol{W}_h^{n+1}+\boldsymbol{W}_h^n)$ in (3.18) and $\boldsymbol{v}=\Delta t(\boldsymbol{S}_h^{n+1}+\boldsymbol{S}_h^{n+1})$ in (3.19), for each q, and add the results. We then use (2.2), the inverse polynomial trace inequality, (2.6), (2.9), the Cauchy-Schwarz and Young's inequalities, continuity and coercivity of the DG bilinear form, and maximise over discrete time just as before. There is this additional term in $F_v(\cdot)$,

$$\sum_{n=0}^{m-1}\sum_{q=1}^{N_\varphi}\varphi_q(e^{-t_{n+1}/\tau_q}+e^{-t_n/\tau_q})a\left(\boldsymbol{u}_0,\boldsymbol{U}_h^{n+1}-\boldsymbol{U}_h^n\right)$$

which can be dealt with by using the fundamental theorem of calculus, summation by parts and continuity. Specifically,

$$\left|\sum_{n=0}^{m-1}\sum_{q=1}^{N_\varphi}\varphi_q(e^{-t_{n+1}/\tau_q}+e^{-t_n/\tau_q})a\left(\boldsymbol{u}_0,\boldsymbol{U}_h^{n+1}-\boldsymbol{U}_h^n\right)\right|$$

$$=\left|2\sum_{q=1}^{N_\varphi}\varphi_q e^{-t_m/\tau_q}a\left(\boldsymbol{u}_0,\boldsymbol{U}_h^m\right)-2\sum_{q=1}^{N_\varphi}\varphi_q e^{-t_0/\tau_q}a\left(\boldsymbol{u}_0,\boldsymbol{U}_h^0\right)\right.$$

$$-\sum_{n=0}^{m-1}\sum_{q=1}^{N_\varphi}\varphi_q(e^{-t_{n+1}/\tau_q}-e^{-t_n/\tau_q})a\left(\boldsymbol{u}_0,\boldsymbol{U}_h^{n+1}+\boldsymbol{U}_h^n\right)\Bigg|$$

$$\leqslant 2\left|a\left(\boldsymbol{u}_0,\boldsymbol{U}_h^m\right)\right|+2\left|a\left(\boldsymbol{u}_0,\boldsymbol{U}_h^0\right)\right|+2K\sum_{q=1}^{N_\varphi}\varphi_q\sum_{n=0}^{m-1}\int_{t_n}^{t_{n+1}}\frac{e^{-t'/\tau_q}}{\tau_q}\left\|\boldsymbol{u}_0\right\|_V\left\|\boldsymbol{U}_h^n\right\|_V dt',$$

since $|e^{-t/\tau_q}|\leqslant 1$, $\forall t\geqslant 0$ for each q and $\sum_{q=1}^{N_\varphi}\varphi_q\leqslant 1$. Young's inequality, continuity and maximising over time now yield an m-independent upper bound. The proof is now completed in a similar way (appropriate choice of Young's inequality constants, and large enough α_0) to the proof of Theorem 4.1. □

As we have already touched upon above, the h^{-1} factor appearing in Theorems 4.1 and 4.2 can be removed by using the results in [5], under their Assumption 2.1 on the quality of the family of meshes. These assumptions require shape regularity, and contact regularity. The former is well understood, and the latter says, essentially, that in $\mathbb{R}^d$, for $d=2$ $(d=3)$ the length (area) of an edge (face) can be bounded below by Ch^{d-1} where h is the local mesh size. The consequence is that $h_{\text{edge}}\sim h_{\text{element}}$. There is a third assumption regarding the existence of a sub-mesh. This is described as a purely technical assumption which allows the proofs to go through with a high degree of generality. For $d=2,3$ they point to the related earlier results of Brenner in [3]. We refer back to [5, Assumption 2.1] for the full details and here just outline the relevant result and give the implications for the improvements in Theorems 4.1 and 4.2.

For a constant, C_{BT}, independent of h, Equation (4.6) in [5] gives

$$\|\boldsymbol{v}\|_{L_q(\partial\Omega)}\leqslant C_{\text{BT}}\left(\|\boldsymbol{v}\|_{L_1(\Omega)}+\|\nabla\boldsymbol{v}\|_{L_p(\Omega)}+\alpha\left(\int_{\Gamma_h}h^{1-p}|[\boldsymbol{v}]|^p\,ds\right)^{1/p}\right)$$

where $\alpha>0$ and we can take $p=2$ with $q=\infty$ $(q=4)$ for $d=2$ $(d=3)$. Using (2.2) and (2.5), with the positivity of the material constants, we can then introduce the DG norm, $\|\cdot\|_V$ into the right hand side above.

Corollary 4.1 (to Theorems 4.1 and 4.2). *With the techniques and result from [5] just discussed, the terms* $h^{-1}\|\boldsymbol{g}_N\|_{H^1(0,T;L_2(\Gamma_N))}^2$ *in Theorems 4.1 and 4.2 can be replaced with* $\|\boldsymbol{g}_N\|_{H^1(0,T;L_2(\Gamma_N))}^2$.

Proof. By $\beta_0(d-1)=1$ in (2.5), recalling (2.2), we get, for a generic constant C,

$$\|\boldsymbol{v}\|_{L_q(\partial\Omega)}\leqslant C\left(\|\boldsymbol{v}\|_{L_1(\Omega)}+\|\nabla\boldsymbol{v}\|_{L_2(\Omega)}+\alpha\left(\int_{\Gamma_h}h^{-1}|[\boldsymbol{v}]|^2\,ds\right)^{1/2}+\alpha\left(\int_{\Gamma_D}h^{-1}|[\boldsymbol{v}]|^2\,ds\right)^{1/2}\right),$$

$$\leqslant C\|\boldsymbol{v}\|_V \tag{4.7}$$

for all $\boldsymbol{v}\in\boldsymbol{\mathcal{D}}_k(\mathcal{E}_h)$. Therefore, for $q=4$ or $q=\infty$ we have $\|\boldsymbol{v}\|_{L_2(\partial\Omega)}\lesssim\|\boldsymbol{v}\|_{L_q(\partial\Omega)}\lesssim\|\boldsymbol{v}\|_V$ which can be used in place of (4.3) above with no need to introduce h^{-1}. □

Again, we emphasise that obtaining these improved results requires lengthy and non-trivial arguments which it would not be appropriate to try and replicate here. The full details are of course in [5].

5 Error Analysis

In order to carry out an *a priori* error analysis we take the usual approach of splitting the error into 'spatial' and 'temporal' components by using the elliptic projection. To this end, define

$$\boldsymbol{\theta}(t):=\boldsymbol{u}(t)-\boldsymbol{R}\boldsymbol{u}(t),\quad\boldsymbol{\vartheta}_q(t):=\boldsymbol{\psi}_q(t)-\boldsymbol{R}\boldsymbol{\psi}_q(t),\quad\boldsymbol{\nu}_q(t):=\boldsymbol{\zeta}_q(t)-\boldsymbol{R}\boldsymbol{\zeta}_q(t),$$

$$\boldsymbol{\chi}^n := \boldsymbol{U}_h^n - \boldsymbol{R}\boldsymbol{u}^n, \qquad \boldsymbol{\varpi}^n := \boldsymbol{W}_h^n - \boldsymbol{R}\dot{\boldsymbol{u}}^n, \quad \varsigma_q^n := \boldsymbol{\Psi}_{hq}^n - \boldsymbol{R}\psi_q^n,$$

$$\boldsymbol{\Upsilon}_q^n := \boldsymbol{S}_{hq}^n - \boldsymbol{R}\boldsymbol{\zeta}_q^n, \quad \text{and} \quad \boldsymbol{\mathcal{E}}_1(t) := \frac{\ddot{\boldsymbol{u}}(t+\Delta t) + \ddot{\boldsymbol{u}}(t)}{2} - \frac{\dot{\boldsymbol{u}}(t+\Delta t) - \dot{\boldsymbol{u}}(t)}{\Delta t},$$

for $t \in [0,T]$, $q = 1, \ldots, N_\varphi$, and $n = 0, \ldots, N$, and note that (3.12) implies that

$$\frac{\boldsymbol{\chi}^{n+1} - \boldsymbol{\chi}^n}{\Delta t} = \frac{\boldsymbol{\varpi}^{n+1} + \boldsymbol{\varpi}^n}{2} - \boldsymbol{\mathcal{E}}_2^n - \boldsymbol{\mathcal{E}}_3^n, \tag{5.1}$$

for $n = 0, \ldots, N-1$ where

$$\boldsymbol{\mathcal{E}}_2(t) := \frac{\dot{\boldsymbol{\theta}}(t+\Delta t) + \dot{\boldsymbol{\theta}}(t)}{2} - \frac{\boldsymbol{\theta}(t+\Delta t) - \boldsymbol{\theta}(t)}{\Delta t},$$

$$\boldsymbol{\mathcal{E}}_3(t) := \frac{\boldsymbol{u}(t+\Delta t) - \boldsymbol{u}(t)}{\Delta t} - \frac{\dot{\boldsymbol{u}}(t+\Delta t) + \dot{\boldsymbol{u}}(t)}{2}.$$

Also, for a three-times time-differentiable function, $\boldsymbol{v}(t)$, with $\boldsymbol{v}^{(3)}$ denoting the third time derivative, we have

$$\frac{\dot{\boldsymbol{v}}(t_{n+1}) + \dot{\boldsymbol{v}}(t_n)}{2} - \frac{\boldsymbol{v}(t_{n+1}) - \boldsymbol{v}(t_n)}{\Delta t} = \frac{1}{2\Delta t} \int_{t_n}^{t_{n+1}} \boldsymbol{v}^{(3)}(t)(t_{n+1} - t)(t - t_n)dt.$$

Hence, if $\boldsymbol{v}^{(3)} \in L_2(t_n, t_{n+1}; \boldsymbol{X})$, the Cauchy-Schwarz inequality gives

$$\left\| \frac{\dot{\boldsymbol{v}}(t_{n+1}) + \dot{\boldsymbol{v}}(t_n)}{2} - \frac{\boldsymbol{v}(t_{n+1}) - \boldsymbol{v}(t_n)}{\Delta t} \right\|_X^2 \leqslant \frac{\Delta t^3}{4} \|\boldsymbol{v}^{(3)}\|_{L_2(t_n, t_{n+1}; X)}^2. \tag{5.2}$$

As is well known, the usual path to an error bound is to use the triangle inequality to split the error using the spatial and temporal components introduced above. The spatial errors are bounded using standard results for elliptic problems, and so it is the temporal error components that demand the bulk of the effort. For our problems, this effort is contained in the next two lemmas: the first for $(\mathbf{D})^h$ and the second for $(\mathbf{V})^h$.

Lemma 5.1. *Suppose* $\boldsymbol{u} \in H^2(0,T; \boldsymbol{C}^2(\Omega)) \cap W_\infty^1(0,T; \boldsymbol{H}^s(\mathcal{E}_h)) \cap H^4(0,T; \boldsymbol{H}^s(\mathcal{E}_h))$ *and* $\beta_0(d-1) \geqslant 1$ *for* $s > 3/2$. *If, for* $n = 0, \ldots, N$, *the solution to* $(\mathbf{D})^h$ *is* $\boldsymbol{U}_h^n, \boldsymbol{W}_h^n, \boldsymbol{\Psi}_{h1}^n, \ldots, \boldsymbol{\Psi}_{hN_\varphi}^n$ *then, for large enough* α_0, *there exists a positive constant* C *such that*

$$\max_{1 \leqslant n \leqslant N} \left\| \boldsymbol{\varpi}^n \right\|_{L_2(\Omega)} + \max_{1 \leqslant n \leqslant N} \left\| \boldsymbol{\chi}^n \right\|_V \leqslant CT \|\boldsymbol{u}\|_{H^4(0,T; H^s(\mathcal{E}_h))} (h^r + \Delta t^2),$$

where $r = \min(k+1, s)$ *and* C *are independent of* h, Δt, T *and the numerical solution.*

Proof. The proof will follow similar arguments in the stability analysis but we additionally use Galerkin orthogonality, the elliptic error estimates (2.10) and (2.11), and the time discretisation error (5.2). Averaging over t_{n+1} and t_n and subtracting (3.8) from (3.13) give

$$\frac{\rho}{\Delta t} \left(\boldsymbol{\varpi}^{n+1} - \boldsymbol{\varpi}^n, \boldsymbol{v} \right) + \frac{1}{2} a \left(\boldsymbol{\chi}^{n+1} + \boldsymbol{\chi}^n, \boldsymbol{v} \right) - \frac{1}{2} \sum_{q=1}^{N_\varphi} a \left(\varsigma_q^{n+1} + \varsigma_q^n, \boldsymbol{v} \right) + \frac{1}{2} J_0^{\alpha_0, \beta_0} \left(\boldsymbol{\varpi}^{n+1} + \boldsymbol{\varpi}^n, \boldsymbol{v} \right)$$

$$= \frac{\rho}{\Delta t} \left(\dot{\boldsymbol{\theta}}^{n+1} - \dot{\boldsymbol{\theta}}^n, \boldsymbol{v} \right) + \rho \left(\boldsymbol{\mathcal{E}}_1^n, \boldsymbol{v} \right), \tag{5.3}$$

$\forall \boldsymbol{v} \in \boldsymbol{\mathcal{D}}_k(\mathcal{E}_h)$ for $0 \leqslant n \leqslant N-1$. In this manner, a subtraction of (3.14) from (3.9) gives

$$\frac{\tau_q}{\Delta t} a \left(\varsigma_q^{n+1} - \varsigma_q^n, \boldsymbol{v} \right) + \frac{1}{2} a \left(\varsigma_q^{n+1} + \varsigma_q^n, \boldsymbol{v} \right) - \frac{\varphi_q}{2} a \left(\boldsymbol{\chi}^{n+1} + \boldsymbol{\chi}^n, \boldsymbol{v} \right) = \tau_q a \left(\boldsymbol{E}_q^n, \boldsymbol{v} \right), \tag{5.4}$$

by Galerkin orthogonality, for any $\boldsymbol{v} \in \boldsymbol{\mathcal{D}}_k(\mathcal{E}_h)$, where

$$\boldsymbol{E}_q(t) = \frac{\dot{\boldsymbol{\psi}}_q(t+\Delta t) + \dot{\boldsymbol{\psi}}_q(t)}{2} - \frac{\boldsymbol{\psi}_q(t+\Delta t) - \boldsymbol{\psi}_q(t)}{\Delta t} \quad \text{for each } q.$$

Inserting $\boldsymbol{v} = 2(\boldsymbol{\chi}^{n+1} - \boldsymbol{\chi}^n)$ into (5.3), with (5.1), and $\boldsymbol{v} = \boldsymbol{\varsigma}_q^{n+1} - \boldsymbol{\varsigma}_q^n$ into (5.4) for each q, summing over $n = 0, \ldots, m-1$ for $m \leqslant N$ gives,

$$
\rho\big\|\boldsymbol{\varpi}^m\big\|_{L_2(\Omega)}^2 + a\left(\boldsymbol{\chi}^m, \boldsymbol{\chi}^m\right) + \sum_{q=1}^{N_\varphi} \frac{1}{\varphi_q} a\left(\boldsymbol{\varsigma}_q^m, \boldsymbol{\varsigma}_q^m\right)
$$

$$
+ \Delta t \sum_{n=0}^{m-1}\sum_{q=1}^{N_\varphi} \frac{2\tau_q}{\varphi_q} a\left(\frac{\boldsymbol{\varsigma}_q^{n+1} - \boldsymbol{\varsigma}_q^n}{\Delta t}, \frac{\boldsymbol{\varsigma}_q^{n+1} - \boldsymbol{\varsigma}_q^n}{\Delta t}\right) + \frac{\Delta t}{2}\sum_{n=0}^{m-1} J_0^{\alpha_0,\beta_0}\left(\boldsymbol{\varpi}^{n+1} + \boldsymbol{\varpi}^n, \boldsymbol{\varpi}^{n+1} + \boldsymbol{\varpi}^n\right)
$$

$$
= \rho\big\|\boldsymbol{\varpi}^0\big\|_{L_2(\Omega)}^2 + a\left(\boldsymbol{\chi}^0, \boldsymbol{\chi}^0\right) + \rho\sum_{n=0}^{m-1}\left(\dot{\boldsymbol{\theta}}^{n+1} - \dot{\boldsymbol{\theta}}^n, \boldsymbol{\varpi}^{n+1} + \boldsymbol{\varpi}^n\right)
$$

$$
- 2\rho\sum_{n=0}^{m-1}\left(\dot{\boldsymbol{\theta}}^{n+1} - \dot{\boldsymbol{\theta}}^n, \boldsymbol{\mathcal{E}}_2^n\right) - 2\rho\sum_{n=0}^{m-1}\left(\dot{\boldsymbol{\theta}}^{n+1} - \dot{\boldsymbol{\theta}}^n, \boldsymbol{\mathcal{E}}_3^n\right)
$$

$$
+ 2\rho\Delta t\sum_{n=0}^{m-1}\left(\boldsymbol{\mathcal{E}}_1^n, \boldsymbol{\varpi}^{n+1} + \boldsymbol{\varpi}^n\right) - \rho\Delta t\sum_{n=0}^{m-1}\left(\boldsymbol{\mathcal{E}}_1^n, \boldsymbol{\mathcal{E}}_2^n\right) - 2\rho\Delta t\sum_{n=0}^{m-1}\left(\boldsymbol{\mathcal{E}}_1^n, \boldsymbol{\mathcal{E}}_3^n\right)
$$

$$
+ 2\rho\sum_{n=0}^{m-1}\left(\boldsymbol{\varpi}^{n+1} - \boldsymbol{\varpi}^n, \boldsymbol{\mathcal{E}}_2^n\right) + 2\rho\sum_{n=0}^{m-1}\left(\boldsymbol{\varpi}^{n+1} - \boldsymbol{\varpi}^n, \boldsymbol{\mathcal{E}}_3^n\right)
$$

$$
+ 2\sum_{q=1}^{N_\varphi} a\left(\boldsymbol{\chi}^m, \boldsymbol{\varsigma}_q^m\right) + \sum_{q=1}^{N_\varphi} \frac{2\tau_q}{\varphi_q} a\left(\boldsymbol{E}_q^{m-1}, \boldsymbol{\varsigma}_q^m\right) - \sum_{n=0}^{m-1}\sum_{q=1}^{N_\varphi} \frac{2\tau_q}{\varphi_q} a\left(\boldsymbol{E}_q^{n+1} - \boldsymbol{E}_q^n, \boldsymbol{\varsigma}_q^{n+1}\right),
$$

when we apply summation by parts to the summation terms from (5.4) with the fact $\boldsymbol{\varsigma}_q^0 = \boldsymbol{0}$, $\forall q$. Hence the definition of DG bilinear form and its coercivity imply that

$$
\rho\big\|\boldsymbol{\varpi}^m\big\|_{L_2(\Omega)}^2 + \big\|\boldsymbol{\chi}^m\big\|_V^2 + \sum_{q=1}^{N_\varphi} \frac{1}{\varphi_q}\big\|\boldsymbol{\varsigma}_q^m\big\|_V^2 + \Delta t\sum_{n=0}^{m-1}\sum_{q=1}^{N_\varphi} \frac{2\kappa\tau_q}{\varphi_q}\left\|\frac{\boldsymbol{\varsigma}_q^{n+1} - \boldsymbol{\varsigma}_q^n}{\Delta t}\right\|^2
$$

$$
+ \frac{\Delta t}{2}\sum_{n=0}^{m-1} J_0^{\alpha_0,\beta_0}\left(\boldsymbol{\varpi}^{n+1} + \boldsymbol{\varpi}^n, \boldsymbol{\varpi}^{n+1} + \boldsymbol{\varpi}^n\right)
$$

$$
\leqslant \Bigg| \rho\big\|\boldsymbol{\varpi}^0\big\|_{L_2(\Omega)}^2 + \big\|\boldsymbol{\chi}^0\big\|_V^2 + \rho\sum_{n=0}^{m-1}\left(\dot{\boldsymbol{\theta}}^{n+1} - \dot{\boldsymbol{\theta}}^n, \boldsymbol{\varpi}^{n+1} + \boldsymbol{\varpi}^n\right)
$$

$$
- 2\rho\sum_{n=0}^{m-1}\left(\dot{\boldsymbol{\theta}}^{n+1} - \dot{\boldsymbol{\theta}}^n, \boldsymbol{\mathcal{E}}_2^n\right) - 2\rho\sum_{n=0}^{m-1}\left(\dot{\boldsymbol{\theta}}^{n+1} - \dot{\boldsymbol{\theta}}^n, \boldsymbol{\mathcal{E}}_3^n\right)
$$

$$
+ \rho\Delta t\sum_{n=0}^{m-1}\left(\boldsymbol{\mathcal{E}}_1^n, \boldsymbol{\varpi}^{n+1} + \boldsymbol{\varpi}^n\right) - 2\rho\Delta t\sum_{n=0}^{m-1}\left(\boldsymbol{\mathcal{E}}_1^n, \boldsymbol{\mathcal{E}}_2^n\right) - 2\rho\Delta t\sum_{n=0}^{m-1}\left(\boldsymbol{\mathcal{E}}_1^n, \boldsymbol{\mathcal{E}}_3^n\right)
$$

$$
+ 2\rho\sum_{n=0}^{m-1}\left(\boldsymbol{\varpi}^{n+1} - \boldsymbol{\varpi}^n, \boldsymbol{\mathcal{E}}_2^n\right) + 2\rho\sum_{n=0}^{m-1}\left(\boldsymbol{\varpi}^{n+1} - \boldsymbol{\varpi}^n, \boldsymbol{\mathcal{E}}_3^n\right)
$$

$$
+ 2\sum_{q=1}^{N_\varphi} a\left(\boldsymbol{\chi}^m, \boldsymbol{\varsigma}_q^m\right) + \sum_{q=1}^{N_\varphi} \frac{2\tau_q}{\varphi_q} a\left(\boldsymbol{E}_q^{m-1}, \boldsymbol{\varsigma}_q^m\right) - \sum_{n=0}^{m-1}\sum_{q=1}^{N_\varphi} \frac{2\tau_q}{\varphi_q} a\left(\boldsymbol{E}_q^{n+1} - \boldsymbol{E}_q^n, \boldsymbol{\varsigma}_q^{n+1}\right)
$$

$$
+ 2\sum_{e\subset\Gamma_h\cup\Gamma_D}\int_e \{\underline{\boldsymbol{D}}\underline{\varepsilon}(\boldsymbol{\chi}^m)\} : [\boldsymbol{\chi}^m \otimes \boldsymbol{n}_e] de + \sum_{q=1}^{N_\varphi}\frac{2}{\varphi_q}\sum_{e\subset\Gamma_h\cup\Gamma_D}\int_e \{\underline{\boldsymbol{D}}\underline{\varepsilon}(\boldsymbol{\varsigma}_q^m)\} : [\boldsymbol{\varsigma}_q^m \otimes \boldsymbol{n}_e] de \Bigg|. \qquad (5.5)
$$

Using the elliptic projection, (3.15), (3.16) and initial conditions, we have $\big\|\boldsymbol{\varpi}^0\big\|_{L_2(\Omega)} \leqslant \big\|\dot{\boldsymbol{\theta}}^0\big\|_{L_2(\Omega)}$ and $\big\|\boldsymbol{\chi}^0\big\|_V = 0$. Further, we note that the fundamental theorem of calculus allows us to deal with the time differences with expressions like $\dot{\boldsymbol{\theta}}^{n+1} - \dot{\boldsymbol{\theta}}^n = \int_{t_n}^{t_{n+1}} \ddot{\boldsymbol{\theta}}(t')dt'$, and then using (5.2) we can bound $\boldsymbol{\mathcal{E}}_1^n, \boldsymbol{\mathcal{E}}_2^n, \boldsymbol{\mathcal{E}}_3^n$

and $\boldsymbol{E}_q^n$, for all n and for each q, in an optimal way. For example,

$$
\left|\Delta t \sum_{n=0}^{m-1} (\boldsymbol{\mathcal{E}}_1^n, \boldsymbol{\mathcal{E}}_2^n)\right| \leqslant \frac{\Delta t}{2} \sum_{n=0}^{N-1} \left\|\boldsymbol{\mathcal{E}}_1^n\right\|_{L_2(\Omega)}^2 + \frac{\Delta t}{2} \sum_{n=0}^{N-1} \left\|\boldsymbol{\mathcal{E}}_2^n\right\|_{L_2(\Omega)}^2
$$
$$
\leqslant \frac{\Delta t^4}{8} \left\|\boldsymbol{u}^{(4)}\right\|_{L_2(0,T;L_2(\Omega))}^2 + \frac{\Delta t^4}{8} \left\|\boldsymbol{\theta}^{(3)}\right\|_{L_2(0,T;L_2(\Omega))}^2,
$$

by the Cauchy-Schwarz inequality, Young's inequality and (5.2). On the other hand, the elliptic error estimates such as (2.11) provide spatial error estimates for $\boldsymbol{\theta}(t)$ and its time derivatives and, noting that the internal variables are analogues of displacement, $\boldsymbol{u}$, we can employ elliptic error estimates for the internal variables as well. Therefore, in the same way as for the stability estimate, using the Cauchy-Schwarz and Young's inequalities, (2.9), summation by parts, maximising in time, and choosing large enough penalty parameters, we eventually arrive at,

$$
\max_{1\leqslant n\leqslant N}\left\|\boldsymbol{\varpi}^n\right\|_{L_2(\Omega)} + \max_{1\leqslant n\leqslant N}\left\|\boldsymbol{\chi}^n\right\|_V + \sum_{q=1}^{N_\varphi} \max_{1\leqslant n\leqslant N}\left\|\boldsymbol{\varsigma}_q^n\right\|_V + \left(\Delta t \sum_{n=0}^{N-1}\sum_{q=1}^{N_\varphi} \frac{\tau_q}{\varphi_q}\left\|\frac{\boldsymbol{\varsigma}_q^{n+1} - \boldsymbol{\varsigma}_q^n}{\Delta t}\right\|^2\right)^{1/2}
$$
$$
+ \left(\Delta t \sum_{n=0}^{N-1} J_0^{\alpha_0,\beta_0}\left(\boldsymbol{\varpi}^{n+1} + \boldsymbol{\varpi}^n, \boldsymbol{\varpi}^{n+1} + \boldsymbol{\varpi}^n\right)\right)^{1/2} \leqslant CT\|\boldsymbol{u}\|_{H^4(0,T;\boldsymbol{H}^s(\mathcal{E}_h))}(h^r + \Delta t^2).
$$

Here C is independent of h, Δt and the solutions, but depends on ρ, Ω, $\partial\Omega$ and the material properties. For full technical details for the proof, we refer to [16]. $\qquad\square$

Next, the analogous estimate for $(\mathbf{V})^h$.

Lemma 5.2. *Suppose $\boldsymbol{u} \in H^2(0,T;\boldsymbol{C}^2(\Omega)) \cap W_\infty^1(0,T;\boldsymbol{H}^s(\mathcal{E}_h)) \cap H^4(0,T;\boldsymbol{H}^s(\mathcal{E}_h))$ and $\beta_0(d-1) \geqslant 1$ for $s > 3/2$. If, for $n = 0,1,\ldots,N$, the solution to $(\mathbf{V})^h$ is $\boldsymbol{U}_h^n$, $\boldsymbol{W}_h^n$, $\boldsymbol{\mathcal{S}}_{h1}^n,\ldots,\boldsymbol{\mathcal{S}}_{hN_\varphi}^n$ then, for large enough α_0, there exists a positive constant C such that*

$$
\max_{1\leqslant n\leqslant N}\left\|\boldsymbol{\varpi}^n\right\|_{L_2(\Omega)} + \max_{1\leqslant n\leqslant N}\left\|\boldsymbol{\chi}^n\right\|_V \leqslant CT\|\boldsymbol{u}\|_{H^4(0,T;H^s(\mathcal{E}_h))}(h^r + \Delta t^2),
$$

where $r = \min(k+1, s)$ and C are independent of h, Δt, T and the numerical solution.

Proof. We follow similar steps as in the proof of Lemma 5.1 for the displacement form to show this claim. By averaging at $t = t_{n+1}$ and $t = t_n$, subtracting (3.10) from (3.18) with $\boldsymbol{v} = 2(\boldsymbol{\chi}^{n+1} - \boldsymbol{\chi}^n)$, and subtracting (3.11) from (3.19), with $\boldsymbol{v} = 2(\boldsymbol{\Upsilon}_q^{n+1} + \boldsymbol{\Upsilon}_q^n)$ for each n and q, summing over $n = 0,\ldots,m-1$ for $m \leqslant N$, employing summation by parts, recalling the coercivity of $a(\cdot,\cdot)$, and using Galerkin orthogonality, we eventually get,

$$
\rho\left\|\boldsymbol{\varpi}^m\right\|_{L_2(\Omega)}^2 + \varphi_0\left\|\boldsymbol{\chi}^m\right\|_V^2 + \sum_{q=1}^{N_\varphi} \frac{\kappa}{\varphi_q}\left\|\boldsymbol{\Upsilon}_q^m\right\|_V^2 + \Delta t \sum_{n=0}^{m-1}\sum_{q=1}^{N_\varphi} \frac{\kappa}{\tau_q\varphi_q}\left\|\boldsymbol{\Upsilon}_q^{n+1} + \boldsymbol{\Upsilon}_q^n\right\|_V^2
$$
$$
+ \frac{\Delta t}{2}\sum_{n=0}^{m-1} J_0^{\alpha_0,\beta_0}\left(\boldsymbol{\varpi}^{n+1} + \boldsymbol{\varpi}^n, \boldsymbol{\varpi}^{n+1} + \boldsymbol{\varpi}^n\right)
$$
$$
\leqslant \left|\rho\left\|\boldsymbol{\varpi}^0\right\|_{L_2(\Omega)}^2 + \varphi_0\left\|\boldsymbol{\chi}^0\right\|_V^2 + \rho\sum_{n=0}^{m-1}\left(\dot{\boldsymbol{\theta}}^{n+1} - \dot{\boldsymbol{\theta}}^n, \boldsymbol{\varpi}^{n+1} + \boldsymbol{\varpi}^n\right)\right.
$$
$$
+ \rho\Delta t\sum_{n=0}^{m-1}\left(\boldsymbol{\mathcal{E}}_1^n, \boldsymbol{\varpi}^{n+1} + \boldsymbol{\varpi}^n\right) - 2\rho\sum_{n=0}^{m-1}\left(\dot{\boldsymbol{\theta}}^{n+1} - \dot{\boldsymbol{\theta}}^n, \boldsymbol{\mathcal{E}}_2^n\right)
$$
$$
- 2\rho\sum_{n=0}^{m-1}\left(\dot{\boldsymbol{\theta}}^{n+1} - \dot{\boldsymbol{\theta}}^n, \boldsymbol{\mathcal{E}}_3^n\right) - 2\rho\Delta t\sum_{n=0}^{m-1}\left(\boldsymbol{\mathcal{E}}_1^n, \boldsymbol{\mathcal{E}}_2^n\right) - 2\rho\Delta t\sum_{n=0}^{m-1}\left(\boldsymbol{\mathcal{E}}_1^n, \boldsymbol{\mathcal{E}}_3^n\right)
$$

$$+ \Delta t \sum_{n=0}^{m-1} \sum_{q=1}^{N_\varphi} \frac{1}{\varphi_q} a \left(\boldsymbol{E}_q^n, \boldsymbol{\Upsilon}_q^{n+1} + \boldsymbol{\Upsilon}_q^n \right) - \Delta t \sum_{n=0}^{m-1} \sum_{q=1}^{N_\varphi} a \left(\boldsymbol{\mathcal{E}}_3^n, \boldsymbol{\Upsilon}_q^{n+1} + \boldsymbol{\Upsilon}_q^n \right)$$

$$+ 2\varphi_0 \sum_{e \subset \Gamma_h \cup \Gamma_D} \int_e \{ \underline{\boldsymbol{D}} \underline{\varepsilon}(\boldsymbol{\chi}^m) \} : [\boldsymbol{\chi}^m \otimes \boldsymbol{n}_e] de \bigg|, \tag{5.6}$$

where

$$\boldsymbol{E}_q(t) := \frac{\dot{\boldsymbol{\zeta}}_q(t + \Delta t) + \dot{\boldsymbol{\zeta}}_q(t)}{2} - \frac{\boldsymbol{\zeta}_q(t + \Delta t) - \boldsymbol{\zeta}_q(t)}{\Delta t} \text{ for each } q.$$

We complete the proof by using the same techniques and results as used earlier: the Cauchy-Schwarz and Young's inequalities, integration and summation by parts, (2.9), (2.11) and (5.2). □

We can now use Lemmas 5.1 and 5.2 to prove the following *a priori* error estimates.

Theorem 5.1 (Error analysis). *Suppose the discrete solutions in $\boldsymbol{\mathcal{D}}_k(\mathcal{E}_h)$ satisfy either $(\mathbf{D})^h$ or $(\mathbf{V})^h$ for integer $s \geqslant 2$, and also that $\boldsymbol{u} \in H^2(0, T; \boldsymbol{C}^2(\Omega)) \cap W^1_\infty(0, T; \boldsymbol{H}^s(\mathcal{E}_h)) \cap H^4(0, T; \boldsymbol{H}^s(\mathcal{E}_h))$. If Lemmas 5.1 and 5.2 hold, then we have*

$$\max_{1 \leqslant n \leqslant N} \left\| \boldsymbol{u}(t_n) - \boldsymbol{U}_h^n \right\|_V \leqslant CT \|\boldsymbol{u}\|_{H^4(0,T;H^s(\mathcal{E}_h))} (h^{r-1} + \Delta t^2),$$

$$\max_{1 \leqslant n \leqslant N} \left\| \boldsymbol{u}(t_n) - \boldsymbol{U}_h^n \right\|_{L_2(\Omega)} \leqslant CT \|\boldsymbol{u}\|_{H^4(0,T;H^s(\mathcal{E}_h))} (h^r + \Delta t^2),$$

$$\max_{1 \leqslant n \leqslant N} \left\| \dot{\boldsymbol{u}}(t_n) - \boldsymbol{W}_h^n \right\|_V \leqslant CT \|\boldsymbol{u}\|_{H^4(0,T;H^s(\mathcal{E}_h))} (h^{r-1} + \Delta t^2),$$

$$\text{and} \quad \max_{1 \leqslant n \leqslant N} \left\| \dot{\boldsymbol{u}}(t_n) - \boldsymbol{W}_h^n \right\|_{L_2(\Omega)} \leqslant CT \|\boldsymbol{u}\|_{H^4(0,T;H^s(\mathcal{E}_h))} (h^r + \Delta t^2),$$

where $r = \min(s + 1, k)$ and C is a positive constant that is independent of h, Δt, T and the exact and discrete solutions, but depends on the polynomial degree k, Ω, $\partial\Omega$, and the material coefficients. Moreover, the initial discrete errors are given by

$$\left\| \boldsymbol{u}_0 - \boldsymbol{U}_h^0 \right\|_V \leqslant Ch^{r-1} \|\|\boldsymbol{u}_0\|\|_{H^s(\mathcal{E}_h)}, \quad \text{and} \quad \left\| \boldsymbol{w}_0 - \boldsymbol{W}_h^0 \right\|_{L_2(\Omega)} \leqslant Ch^r \|\|\boldsymbol{w}_0\|\|_{H^s(\mathcal{E}_h)}.$$

Proof. Using the triangle inequality with Lemmas 5.1 and 5.2, and the DG elliptic error estimates, we get, for any $n \in \{1, \ldots, N\}$, that

$$\left\| \boldsymbol{u}(t_n) - \boldsymbol{U}_h^n \right\|_V \leqslant \left\| \boldsymbol{\theta}(t_n) \right\|_V + \left\| \boldsymbol{\chi}^n \right\|_V \leqslant CT \|\boldsymbol{u}\|_{H^4(0,T;H^s(\mathcal{E}_h))} (h^{r-1} + \Delta t^2). \tag{5.7}$$

Recalling Poincaré's inequality (2.2) indicates that $\left\| \boldsymbol{v} \right\|_{L_2(\Omega)} \leqslant C \left\| \boldsymbol{v} \right\|_V$ for any $\boldsymbol{v} \in \boldsymbol{\mathcal{D}}_k(\mathcal{E}_h)$. Hence we have

$$\left\| \boldsymbol{u}(t_n) - \boldsymbol{U}_h^n \right\|_{L_2(\Omega)} \leqslant \left\| \boldsymbol{\theta}(t_n) \right\|_{L_2(\Omega)} + C \left\| \boldsymbol{\chi}^n \right\|_V \leqslant CT \|\boldsymbol{u}\|_{H^4(0,T;H^s(\mathcal{E}_h))} (h^{r-1} + \Delta t^2). \tag{5.8}$$

In a similar way, we have

$$\left\| \dot{\boldsymbol{u}}(t_n) - \boldsymbol{W}_h^n \right\|_{L_2(\Omega)} \leqslant \left\| \dot{\boldsymbol{\theta}}(t_n) \right\|_{L_2(\Omega)} + \left\| \boldsymbol{\varpi}^n \right\|_{L_2(\Omega)} \leqslant CT \|\boldsymbol{u}\|_{H^4(0,T;H^s(\mathcal{E}_h))} (h^r + \Delta t^2). \tag{5.9}$$

On the other hand, as seen in (5.5) and (5.6), the jump penalty term of $\boldsymbol{\varpi}^n$ is also bounded by the same upper bound. In other words, we have

$$\left(J_0^{\alpha_0, \beta_0} \left(\boldsymbol{\varpi}^n, \boldsymbol{\varpi}^n \right) \right)^{1/2} = O(h^r + \Delta t^2). \tag{5.10}$$

Using this argument with the inverse inequality (2.3), we can derive energy norm error estimates for the velocity vector field and get,

$$\left\| \dot{\boldsymbol{u}}(t_n) - \boldsymbol{W}_h^n \right\|_V \leqslant \left\| \dot{\boldsymbol{\theta}}(t_n) \right\|_V + \left\| \boldsymbol{\varpi}^n \right\|_V \leqslant \left\| \dot{\boldsymbol{\theta}}(t_n) \right\|_V + Ch^{-1} \left\| \boldsymbol{\varpi}^n \right\|_{L_2(\Omega)} + \left(J_0^{\alpha_0, \beta_0} \left(\boldsymbol{\varpi}^n, \boldsymbol{\varpi}^n \right) \right)^{1/2}$$

$$\leqslant CT \|\boldsymbol{u}\|_{H^4(0,T;H^s(\mathcal{E}_h))} (h^{r-1} + \Delta t^2). \tag{5.11}$$

Since n is arbitrary and the the right hand sides of (5.7)-(5.11) are independent of n, the proof is completed. Furthermore, to show the discrete errors for $n = 0$, we want to use the triangular inequalities, DG elliptic error estimates and initial (DG elliptic/L_2) projections, e.g. (3.15) and (3.16). Hence we have

$$\left\| \boldsymbol{u}_0 - \boldsymbol{U}_h^0 \right\|_V = \left\| \boldsymbol{\theta}(0) - \boldsymbol{\chi}^0 \right\|_V \leqslant \left\| \boldsymbol{\theta}(0) \right\|_V + \left\| \boldsymbol{\chi}^0 \right\|_V = \left\| \boldsymbol{\theta}(0) \right\|_V \leqslant Ch^{r-1} \| \boldsymbol{u}_0 \|_{H^s(\mathcal{E}_h)},$$

by the fact $\left\| \boldsymbol{\chi}^0 \right\|_V = 0$ and (2.10). Also, since $\left\| \boldsymbol{\varpi}^0 \right\|_{L_2(\Omega)} \leqslant \left\| \dot{\boldsymbol{\theta}}(0) \right\|_{L_2(\Omega)}$, (2.11) leads to

$$\left\| \boldsymbol{w}_0 - \boldsymbol{W}_h^0 \right\|_{L_2(\Omega)} = \left\| \dot{\boldsymbol{\theta}}(0) - \boldsymbol{\varpi}^0 \right\|_{L_2(\Omega)} \leqslant \left\| \dot{\boldsymbol{\theta}}(0) \right\|_{L_2(\Omega)} + \left\| \boldsymbol{\varpi}^0 \right\|_{L_2(\Omega)} \leqslant 2 \left\| \dot{\boldsymbol{\theta}}(0) \right\|_{L_2(\Omega)} \leqslant Ch^r \| \boldsymbol{w}_0 \|_{H^s(\mathcal{E}_h)}.$$

$\square$

6 Numerical Experiments

In this section we use the FEniCS environment, see [1] and https://fenicsproject.org, to give the results of some numerical experiments that were carried out to demonstrate the convergence rates proven above: we present tables of numerical errors, as well as convergence rates. The python codes to reproduce these results are available at Jang's Github (https://github.com/Yongseok7717/Visco_Int_CG), and can be used to reproduce the results that are given below. Alternatively, these results can also be reproduced by using docker. In this case the commands to run are:

```
docker pull jangyour/fenics_fem
docker run -ti jangyour/fenics_fem
cd  visco/Int_DG; . main.sh
```

An exact solution
As is common, we use an artificial, or *manufactured*, exact solution in order to calculate the errors. Let this manufactured strong solution be

$$\boldsymbol{u}(x, y, t) = \begin{bmatrix} xye^{1-t} \\ \cos(t)\sin(xy) \end{bmatrix} \in C^\infty(0, T; \boldsymbol{C}^\infty(\Omega))$$

where $\Omega = (0, 1)^2$ and $T = 1$. We use two internal variables with coefficients and time delays $\varphi_0 = 0.5$, $\varphi_1 = 0.1$, $\varphi_2 = 0.4$, $\tau_1 = 0.5$, $\tau_2 = 1.5$ and (because we are not constrained by the physical reality here) we assume for simplicity an identity fourth order tensor as our $\boldsymbol{D}$ so that $\boldsymbol{D}\boldsymbol{\varepsilon} = \boldsymbol{\varepsilon}$. We define the Dirichlet boundary as

$$\Gamma_D = \{(x, y) \in \partial\Omega \mid x = 0 \text{ or } y = 0\}$$

and then $\boldsymbol{u} = \boldsymbol{0}$ on Γ_D, and the other data are readily computed.

Numerical results
We present numerical errors to demonstrate the convergence rates given by the theorems and for this we define $\boldsymbol{e}^n = \boldsymbol{u}(t_n) - \boldsymbol{U}_h^n$ and $\tilde{\boldsymbol{e}}^n = \boldsymbol{w}(t_n) - \boldsymbol{W}_h^n$ for $n = 0, \dots, N$. According to Theorem 5.1, we have the L_2 norm error as well as DG energy norm error such that

$$\left\| \boldsymbol{e}^n \right\|_V = O(h^k + \Delta t^2), \text{ and } \left\| \boldsymbol{e}^n \right\|_{L_2(\Omega)} = O(h^{k+1} + \Delta t^2),$$

since $s = \infty$. Also, we have the same rates of convergence for the velocity error. By recalling Korn's inequality (2.7), we note that the broken H^1 norm is bounded by the energy norm. Therefore, we have broken H^1 error estimates such that

$$\left\| \boldsymbol{e}^n \right\|_{H^1(\mathcal{E}_h)} + \left\| \tilde{\boldsymbol{e}}^n \right\|_{H^1(\mathcal{E}_h)} \leqslant C(h^k + \Delta t^2),$$

for some positive constant C. Since the DG energy norm depends on the penalty parameters α_0 and β_0, we hereafter consider the errors in the broken H^1 norm instead.

Firstly, we set $\Delta t = h$ and define the numerical convergence rate d_c by

$$d_c = \frac{\log(\text{error of } h_1) - \log(\text{error of } h_2)}{\log(h_1) - \log(h_2)}.$$

We can see in Figure 1 that d_c is 1 for both the displacement and velocity form errors when $k = 1$, and that it suggests quadratic convergence orders for L_2 norm error or when $k = 2$, regardless of which internal variable form is used.
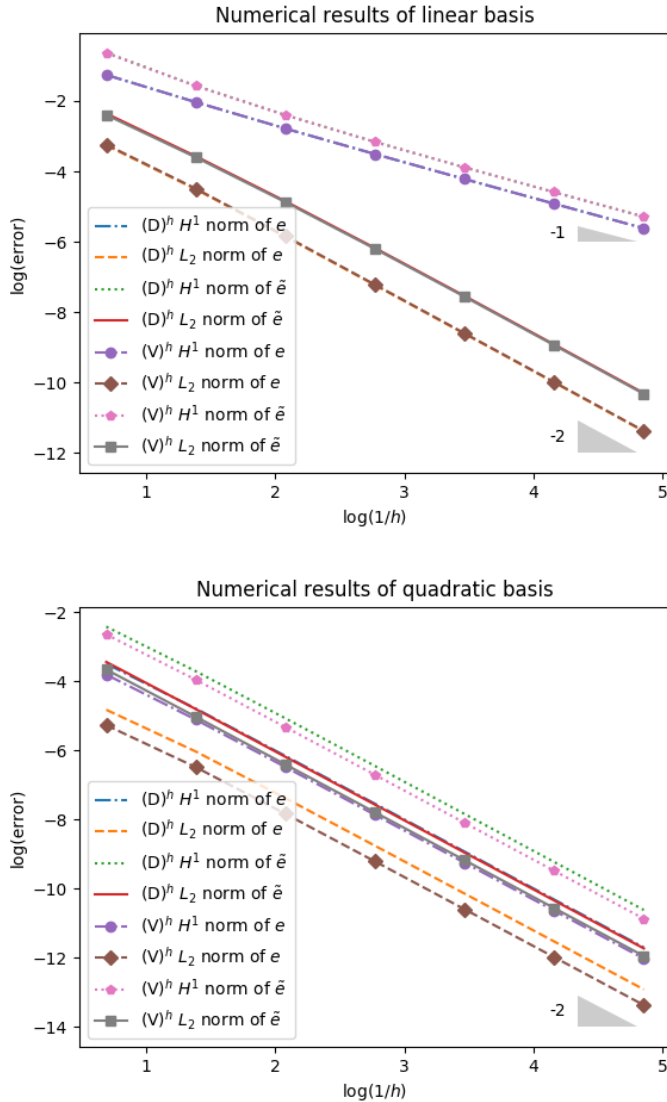
Fig. 1: Numerical convergence order: **linear** (top) and **quadratic** (bottom) polynomial basis

Secondly, if we take $\Delta t \ll h$ we can render the 'time error' negligible in comparison to the 'space error' and isolate the spatial convergence rates. Some example results for this are shown in Tables 1 and 2, where we see that the numerical rates follow the spatial convergence order of $d_c = k$ (resp. $d_c = k + 1$) in the H^1 (resp. L_2) norm. We can also see that there is no significant difference between the numerical schemes $(\mathbf{D})^h$ and $(\mathbf{V})^h$, in terms of convergence rates as well as the size of the errors.

Thirdly, in Table 3 we give some results for when the spatial error became negligibly small to the temporal error, to observe second order accuracy in time regardless of spatial norms, displacement/velocity fields and internal variable forms. All of these results are consistent with the claims in the theorems.

k	h	Displacement form		Velocity form	
		$\||\|e^N\|\||_{H^1(\mathcal{E}_h)}$	$\||\|\tilde{e}^N\|\||_{H^1(\mathcal{E}_h)}$	$\||\|e^N\|\||_{H^1(\mathcal{E}_h)}$	$\||\|\tilde{e}^N\|\||_{H^1(\mathcal{E}_h)}$
	1/4	1.298e-01	1.951e-01	1.298e-01	1.951e-01
1	1/8	6.177e-02 (1.07)	8.741e-02 (1.16)	6.177e-02 (1.07)	8.741e-02 (1.16)
	1/16	2.993e-02 (1.05)	4.130e-02 (1.08)	2.993e-02 (1.05)	4.130e-02 (1.08)
	1/32	1.473e-02 (1.02)	2.001e-02 (1.04)	1.473e-02 (1.02)	2.001e-02 (1.04)
	1/4	3.168e-03	4.996e-03	3.168e-03	4.996e-03
2	1/8	8.030e-04 (1.98)	1.284e-03 (1.96)	8.030e-04 (1.98)	1.284e-03 (1.96)
	1/16	2.008e-04 (2.00)	3.256e-04 (1.98)	2.008e-04 (2.00)	3.256e-04 (1.98)
	1/32	5.010e-05 (2.00)	8.206e-05 (1.99)	5.010e-05 (2.00)	8.206e-05 (1.99)

Tab. 1: H^1 norm of numerical errors (orders) when $\Delta t = 1/2048$

k	h	Displacement form		Velocity form	
		$\|e^N\|_{L_2(\Omega)}$	$\|\tilde{e}^N\|_{L_2(\Omega)}$	$\|e^N\|_{L_2(\Omega)}$	$\|\tilde{e}^N\|_{L_2(\Omega)}$
	1/4	1.067e-02	2.293e-02	1.067e-02	2.293e-02
1	1/8	2.808e-03 (1.93)	6.691e-03 (1.78)	2.808e-03 (1.93)	6.691e-03 (1.78)
	1/16	7.094e-04 (1.98)	1.182e-03 (1.88)	7.094e-04 (1.98)	1.182e-03 (1.88)
	1/32	1.781e-04 (1.99)	4.686e-04 (1.95)	1.781e-04 (1.99)	4.686e-04 (1.95)
	1/4	8.362e-05	1.496e-04	8.362e-05	1.496e-04
2	1/8	1.011e-05 (3.05)	1.861e-05 (3.01)	1.011e-05 (3.05)	1.861e-05 (3.01)
	1/16	1.231e-06 (3.04)	2.315e-06 (3.01)	1.231e-06 (3.04)	2.315e-06 (3.01)
	1/32	1.515e-07 (3.02)	2.906e-07 (3.00)	1.514e-07 (3.02)	2.902e-07 (3.00)

Tab. 2: L_2 norm of numerical errors (orders) when $\Delta t = 1/2048$

Norm	Δt	Displacement form		Velocity form	
		e^N	$\tilde{e}^N$	e^N	$\tilde{e}^N$
	1/2	2.696e-02	9.579e-02	1.766e-02	7.348e-02
H^1	1/4	7.445e-03 (1.86)	2.461e-02 (1.96)	4.879e-03 (1.86)	1.880e-02 (1.97)
	1/8	1.894e-03 (1.97)	6.169e-03 (2.00)	1.2429e-03 (1.97)	4.712e-03 (2.00)
	1/16	4.747e-04 (2.00)	1.549e-04 (2.00)	3.117e-04 (2.00)	1.181e-03 (2.00)
	1/2	8.121e-02	3.222e-02	5.256e-03	2.586e-02
L_2	1/4	2.410e-03 (1.75)	8.221e-03 (1.97)	1.534e-03 (1.78)	6.601e-03 (1.97)
	1/8	6.252e-04 (1.95)	2.067e-03 (1.99)	3.974e-04 (1.95)	1.659e-03 (1.99)
	1/16	1.577e-04 (1.99)	5.178e-04 (2.00)	1.001e-04 (1.99)	4.155e-04 (2.00)

Tab. 3: Time convergence errors (orders) for fixed $h = 1/128$ and $k = 2$

Penalty parameters

For well-posedness as well as optimal convergence, we need to have 'large enough' penalty parameters and following studies of elasticity problems, [14, 25], we took $\alpha_0 = 10$ and $\beta_0 = 1$ for the computations above. If α_0 is small our numerical schemes will lose stability and convergence. This is illustrated in Table 4 where we see that the numerical errors diverged when $\alpha_0 = 0.1$. On the other hand, in order to observe the requirements of the stability and error analyses above we need $\beta_0(d-1) \geqslant 1$ but, a too large β_0 will result in the assembled global matrix being ill-conditioned. Therefore, taking $\beta_0 = 1/(d-1)$ seems to be the most reasonable choice. In fact, the condition number of the assembled system matrix in the interior penalty method is of order $O(h^{-(\beta_0+1)})$ [16, 20], and hence we may encounter difficulty in solving linear systems for large β_0 if we use iterative solvers. For more details, we refer to [16, 20].

q	τ_q (secs)	dyne/cm^2	φ_q
0		2.24×10^7	0.001000236663139
1	0.02	1.94×10^9	0.086627639575435
2	0.20	2.83×10^9	0.126369185566228
3	2	5.54×10^9	0.247379960437068
4	20	6.02×10^9	0.268813603218619
5	200	3.88×10^9	0.173255279150871
6	2000	1.56×10^9	0.069659339040041
7	20000	4.10×10^8	0.018307903209241
8	200000	1.38×10^8	0.006162172299696
9	2000000	3.68×10^7	0.001643245946586
10	20000000	7.90×10^6	0.000352762037446
11	200000000	9.60×10^6	0.000428672855631

Tab. 5: Prony series data for PMMA taken from [19, Table 1]. The second and third columns are from the source, one-tenth of the sum of the third column (because $10\,\text{dyne/cm}^2 = 1\,\text{N/m}^2$) gives $2.23947\,\text{GN/m}^2$, and the fourth column is the normalization of one-tenth of the third column (to ensure that $\varphi(0) = 1$ in (1.6)).

	Displacement form			Velocity form		
h	1/2	1/4	1/8	1/2	1/4	1/8
Error	2.262	9.527e+03	1.262e+14	2.286	9.364e+03	1.266e+14

Tab. 4: $\left\| e^N \right\|_{L_2(\Omega)}$ for $\alpha_0 = 0.1$ where $\Delta t = h$ and $k = 1$

An example with real material data

The results above are based on artificial choices of the material data — the point was merely to show convergence, and illustrate the estimates. In this closing section we illustrate the displacement formulation using real material data for PMMA (polymethyl methacrylate), taken from [19, Table 1]. The demonstration given below shows clearly the effect of viscoelastic damping on the longer time response.

First, the Prony series relaxation data from [19, Table 1] are converted from dyne/cm^2 to N/m^2 by dividing by ten, and then the coefficients are normalized (and nondimensionalized) to fit our assumptions for (1.6). The results of this are in Table 5. The stiffness modulus resulting from this normalization turns out to be $E = 2.23947\,\text{GN/m}^2$ and is absorbed into the tensor $\underline{\underline{D}}$ in (1.5). We assume a compressible isotropic homogeneous medium and so this tensor, in two space dimensions, has a matrix representation as

$$\underline{\underline{D}} = \begin{pmatrix} \lambda + 2\mu & \lambda & 0 \\ \lambda & \lambda + 2\mu & 0 \\ 0 & 0 & \mu \end{pmatrix} \quad \text{with} \quad \underline{\sigma} = \begin{pmatrix} \sigma_{11} \\ \sigma_{22} \\ \sigma_{12} \end{pmatrix} \quad \text{and} \quad \underline{\varepsilon} = \begin{pmatrix} \varepsilon_{11} \\ \varepsilon_{22} \\ 2\varepsilon_{12} \end{pmatrix}$$

for Lamé parameters $\lambda = \nu E / \big((1+\nu)(1-2\nu)\big)$ and $\mu = \frac{1}{2}E/(1+\nu)$ (see e.g. [9, 12, 11, 17, 6]). We assume from, for example, [2] a Poisson's ratio of $\nu = 0.35$ and a mass density of $\rho = 1190\,\text{kg/m}^3$.

We take $\Omega = (0,2) \times (0,1)$ with zero initial data and solve over $(0,T) = (0,0.3)$. There are homogeneous boundary conditions of Dirichlet type on the left side and homogeneous Neumann conditions on the top and bottom edges. The body force, $\boldsymbol{f}$, in (1.1) is zero. On the right hand edge of the domain we impose the traction

$$\boldsymbol{g}(\boldsymbol{x},t) = \begin{pmatrix} g_1(\boldsymbol{x},t) \\ 0 \end{pmatrix} \text{N/m}^2 \quad \text{where} \quad g_1(\boldsymbol{x},t) = A\mathcal{H}(0.01) \tag{6.1}$$

for $A = 50\,\text{MN/m}^2$ and where $\mathcal{H}$ denotes the Heaviside step. The finite element space is piecewise quadratic with an $N_x \times N_y$ uniform spatial mesh of right-angled triangles (diagonals from North-West to South-East), and we use N_t time steps of size $\Delta T = T/N_t$. We took $\alpha = 10$ and $\beta = 1$, and scaled the entire discrete system by dividing through by 10^9: this was needed to prevent runtime precision errors being thrown by the linear solvers.
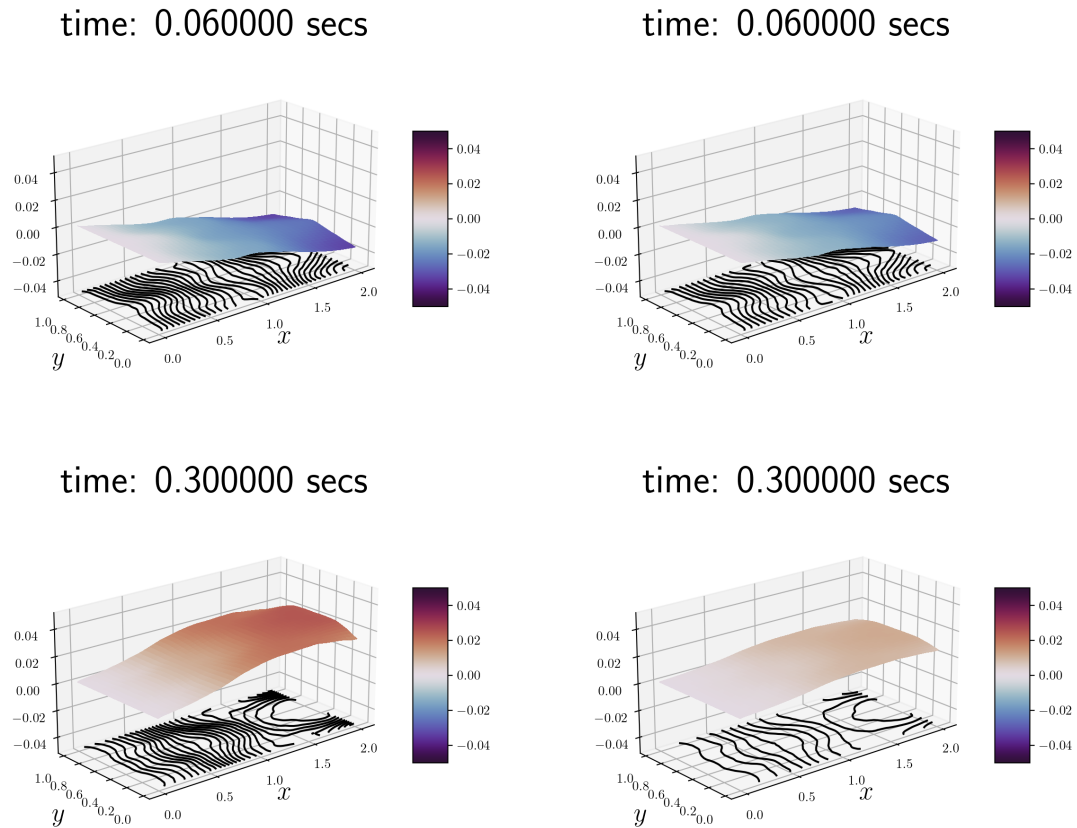
Fig. 2: Snapshots at $t = 0.06$ s and $t = 0.3$ s of the discrete solution u_1 for the linear elasticity problem on the left and the viscoelastic problem on the right. Here $N_x \times N_y = 120 \times 60$ with $N_t = 24000$.

We give two different solutions to compare elastic and viscoelastic short time response to the traction. The elastic solution is generated by setting $\varphi_q = 0$ for $q = 1, \ldots, 11$, and setting $\varphi_0 = 1$. The results for the u_1 displacement are shown as surface plots in Figure 2 for $t = 0.06$ s and $t = 0.3$ s. The similarity at the shorter time, as well as the viscoelastic decay at the longer time is evident. To see this more clearly the pointwise displacement $u_1(2, 0.5)$ is shown in Figure 3.

The code that produced these results can be obtained from

https://github.com/variationalform/SIPG_PMMA_demo_2022

with `git clone git@github.com:variationalform/SIPG_PMMA_demo_2022.git`. Or, one can generate the results in a docker container from

https://hub.docker.com/r/variationalform/fem

with

```
docker pull variationalform/fem:SIPG_PMMA_demo_2022
docker run -ti variationalform/fem:SIPG_PMMA_demo_2022
# in the container
cd runtime/le
./longrun_le.sh | tee ./longrun_le_out.txt
```
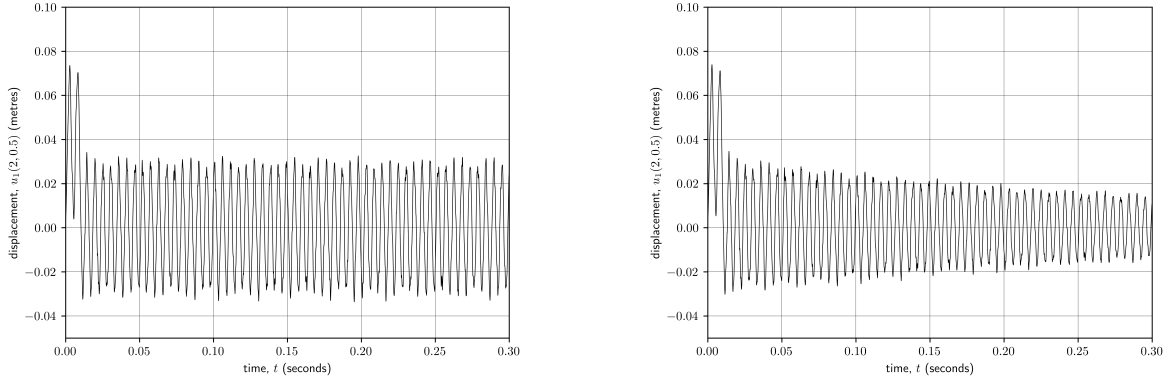
Fig. 3: Plots of the discrete solution $u_1(2, 0.5)$ for the linear elasticity problem on the left and the viscoelastic problem on the right. Here $N_x \times N_y = 120 \times 60$ with $N_t = 24000$.

for the linear elastic runs. Alter `le` to `ve` to run with the viscoelastic data. This docker image uses FEniCS with dolfin version 2017.2.0.

7 Conclusion and Discussion

We have presented an *a priori* stability and error analysis of the DGFEM for linear dynamic viscoelasticity with two types of internal variables used to replace the fading memory Volterra integral. We have given illustrative numerical results, explained how these results can be reproduced, and we have observed that both of the schemes (for each type of internal variable) behaves similarly. The numerics are consistent with the predicted convergence rates.

   The main achievement of this work is that we have been able to give the stability and error bounds without recourse to Grönwall's inequality, with the result that the stability and error bounds depend explicitly on the final time linearly, and not exponentially, (along with the time dependence in the exact solution norms). This is a significant improvement over the estimates given in [22]. Moreover, the schemes presented here use displacement or velocity internal variables rather than stresses, and so — compared to [22] — for the schemes presented here, there is a modest reduction in the computer memory requirements.

   An inspection of Tables 1, 2 and 3 indicates that there is no particular reason to prefer one formulation over the other. This is perhaps not surprising, but we are not aware of any previous work that has demonstrated it both in theoretical estimates and in numerical experiments. We return to this point below.

   We assumed throughout that $\varphi_0 > 0$ in (1.6), which is reasonable for materials with long term stiffness ('solids' as defined by Golden and Graham in [12]). However, for 'fluids', under the specific condition $\varphi_0 = 0$, the velocity form will yield an interesting alternative model. In particular, with $\boldsymbol{u}_0 = \boldsymbol{0}$ for simplicity, we can rewrite (3.6) as

$$\rho\dot{\boldsymbol{w}} - \sum_{q=1}^{N_\varphi} \nabla \cdot \left(\underline{\boldsymbol{D}}\underline{\boldsymbol{\varepsilon}}\left(\boldsymbol{\zeta}_q\right)\right) = \boldsymbol{f},$$

where we have set $\dot{\boldsymbol{u}} = \boldsymbol{w}$. The internal variable still evolves according to the ODE, (3.7), which holds at every point in space, and so in the numerical scheme there is no need to introduce displacement. This results in a reduced memory requirement, because in this case we would certainly prefer the velocity formulation. We plan to explore this interesting variant in a future study.

   Finally, the results in Figures 2 and 3 demonstrate that this method can be applied to *real* materials.

References

[1] Alnæs, M., Blechta, J., Hake, J., Johansson, A., Kehlet, B., Logg, A., Richardson, C., Ring, J., Rognes, M. E., and Wells, G. N. The FEniCS project version 1.5. *Archive of Numerical Software 3*, 100 (2015), 9–23.

[2] Bang's Laboratories, Inc. Material properties of polystyrene and poly(methyl methacrylate) (PMMA) microspheres. https://www.bangslabs.com/material-properties-polystyrene-and-polymethyl-methacrylate-pmma-microspheres, 2015. Tech Support Doc 0021. Accessed: 2022-06-12.

[3] Brenner, S. C. Poincaré–Friedrichs inequalities for piecewise H^1 functions. *SIAM Journal on Numerical Analysis 41*, 1 (2003), 306–324.

[4] Brenner, S. C. Korn's inequalities for piecewise H^1 vector fields. *Mathematics of Computation* (2004), 1067–1087.

[5] Buffa, A., and Ortner, C. Compact embeddings of broken Sobolev spaces and applications. *IMA Journal of Numerical Analysis 29*, 4 (2009), 827–855.

[6] Christensen, R. M. *Theory of viscoelasticity: an introduction.* Academic Press, Inc. (London) Ltd., 1971.

[7] Crank, J., and Nicolson, P. A practical method for numerical evaluation of solutions of partial differential equations of the heat-conduction type. *Advances in Computational Mathematics 6*, 1 (Dec 1996), 207–226.

[8] Drozdov, A. D. *Viscoelastic structures: mechanics of growth and aging.* Academic Press, 1998.

[9] Ferry, J. D. *Viscoelastic properties of polymers.* John Wiley and Sons Inc., 1970.

[10] Findley, W. N., and Davis, F. A. *Creep and relaxation of nonlinear viscoelastic materials.* Courier Corporation, 2013.

[11] Findley, W. N., Lai, J. S., and Onaran, K. *Creep and relaxation of nonlinear viscoelastic materials (with an introduction to linear viscoelasticity).* Dover Publications Inc., New York, 1989.

[12] Golden, J. M., and Graham, G. A. *Boundary value problems in linear viscoelasticity.* Springer Science & Business Media, 2013.

[13] Hansbo, P., and Larson, M. G. Discontinuous Galerkin methods for incompressible and nearly incompressible elasticity by Nitsche's method. *Computer methods in applied mechanics and engineering 191*, 17-18 (2002), 1895–1908.

[14] Houston, P., Schötzau, D., and Wihler, T. P. An *hp*-adaptive mixed discontinuous Galerkin FEM for nearly incompressible linear elasticity. *Computer methods in applied mechanics and engineering 195*, 25-28 (2006), 3224–3246.

[15] Hunter, S. C. *Mechanics of continuous media.* Halsted Press, 1976.

[16] Jang, Y. *Spatially Continuous and Discontinuous Galerkin Finite Element Approximations for Dynamic Viscoelastic Problems.* PhD thesis, Brunel University London, 2020. BURA http://bura.brunel.ac.uk/handle/2438/21084.

[17] Lockett, F. J. *Nonlinear viscoelastic solids.* Academic Press, 1972.

[18] Ozisik, S., Riviere, B., and Warburton, T. On the constants in inverse inequalities in L_2. Tech. rep., Rice University, 2010.

[19] Park, S. W., and Schapery, R. A. Methods of interconversion between linear viscoelastic material functions. Part I — a numerical method based on Prony series. *International Journal of Solids and Structures 36* (1999), 1653–1675.

[20] Rivière, B. *Discontinuous Galerkin methods for solving elliptic and parabolic equations: theory and implementation.* SIAM, 2008.

[21] Riviére, B., Shaw, S., Wheeler, M. F., and Whiteman, J. R. Discontinuous Galerkin finite element methods for linear elasticity and quasistatic linear viscoelasticity. *Numerische Mathematik 95*, 2 (2003), 347–376.

[22] RIVIÈRE, B., SHAW, S., AND WHITEMAN, J. Discontinuous Galerkin finite element methods for dynamic linear solid viscoelasticity problems. *Numerical Methods for Partial Differential Equations 23*, 5 (2007), 1149–1166.

[23] SHAW, S., AND WHITEMAN, J. Some partial differential Volterra equation problems arising in viscoelasticity. In *Proceedings of Equadiff* (1998), vol. 9, pp. 183–200.

[24] WARBURTON, T., AND HESTHAVEN, J. On the constants in hp-finite element trace inverse inequalities. *Computer Methods in Applied Mechanics and Engineering 192*, 25 (2003), 2765 – 2773.

[25] WIHLER, T. Locking-free adaptive discontinuous Galerkin FEM for linear elasticity problems. *Mathematics of computation 75*, 255 (2006), 1087–1102.